

**ELUCIDATING THE ROLE OF HUMAN OBG LIKE ATPASE 1 (HOLA1) IN  
APOPTOSIS**

**NIRUJAH BALASINGAM**  
**Bachelor of Science, University of Mysore, 2014**

A Thesis  
Submitted to the School of Graduate Studies  
of the University of Lethbridge  
in Partial Fulfilment of the  
Requirements for the Degree

**MASTER OF SCIENCE**

Department of Chemistry and Biochemistry  
University of Lethbridge  
LETHBRIDGE, ALBERTA, CANADA

© Nirujah Balasingam, 2017

ELUCIDATING THE ROLE OF HUMAN OBG LIKE ATPASE 1 (HOLA1) IN  
APOPTOSIS

NIRUJAH BALASINGAM

Date of Defense: December 07, 2017

Dr. N. Thakor Supervisor	Assistant Professor	Ph.D.
Dr. H. J. Wieden Co-Supervisor	Professor	Ph.D.
Dr. M. Roussel Thesis Examination Committee Member	Professor	Ph.D.
Dr. T. Russell Thesis Examination Committee Member	Associate Professor	Ph.D.
Dr. A. Gorrell External examiner University of Northern British Columbia British Columbia	Associate Professor	Ph.D.
Dr. P. G. Hayes Chair, Thesis Examination Committee	Professor	Ph.D.

## **Dedication**

***This thesis is dedicated to my beloved family,***

*I am grateful for my Parents and Siblings for the endless love and faith in me.*

*Special thanks to my brother for being my pillar of strength, a constant source of knowledge and inspiration for me.*

***Thank you, Anna,***

*I am also grateful to my sister-in-law for the support and guidance*

*& finally, the joy of my life,*

*My cute little Nephews and Niece*

*Without you all I am nothing.*

## **Abstract**

hOLA1 is a purine nucleotide binding protein that belongs to the P-loop GTPase family. hOLA1 suppresses protein synthesis by limiting ternary complex formation thus promoting the integrated stress response (ISR). ISR determines cell fate by activating or inhibiting pro- and anti-apoptotic proteins depending on the type of the stress condition. ISR facilitates cell survival in response to mild stress and promotes apoptosis in response to chronic stress. Depletion of hOLA1 leads to increased cell survival and diminished ISR. This study investigates the role of hOLA1 in apoptosis. My hypothesis was that diminished ISR in hOLA1-depleted cells leads to upregulation of anti-apoptotic proteins thus inhibiting apoptosis. Indeed, this study shows that hOLA1 depletion upregulates anti-apoptotic proteins such as cIAP1, cIAP2, and Bcl-xL, thus inhibiting apoptosis. The inhibition of apoptosis was studied by assessing caspase activation, cleaved poly (ADP-ribose) polymerase (PARP) level, and measuring apoptosis by propidium iodide (PI) staining and flow cytometry.

## **Acknowledgment**

First, I would like to thank my supervisor Dr. Nehal Thakor for his constant guidance and support throughout this journey. Next, special thanks to my co-supervisor Dr. Hans-Joachim Wieden for the collaboration.

I wish to thank my committee members Dr. Marc Roussel and Dr. Tony Russell for the valuable comments and guidance. Finally, I would like to thank my lab members for the great support during my master's program.

## Table of Contents

List of Tables .....	vii
List of Figures .....	viii
Abbreviations .....	ix
Chapter 1: Introduction .....	1
1.1 Overview of eukaryotic gene expression .....	1
1.1.1 Cap-dependent translation.....	1
1.1.2 Cap-independent translation.....	5
1.1.3 Regulation of translation and integrated stress response.....	6
1.2 Activation and termination of the ISR .....	8
1.3 Apoptosis and programmed cell death .....	11
1.3.1 Mitochondrial or intrinsic apoptotic pathway .....	12
1.3.2 Extrinsic pathway .....	13
1.3.3 Regulation of apoptosis .....	15
1.4 Role of translational control in cancer .....	17
1.5 Human obg like ATPase 1 (hOLA1).....	18
1.5.1 hOLA1 as a regulator of protein synthesis and ISR .....	19
1.5.2 hOLA1 as a cell cycle regulator Regulation of apoptosis .....	20
1.6 Aim of the project .....	22
Chapter 2: Materials and methods .....	23
2.1 Cell lines .....	23
2.2 Transfection .....	23
2.3 Western blotting.....	24
2.4 alamarBlue™ assay.....	26
2.5 Propidium iodide (PI) staining and flow cytometry .....	26
2.6 Immunoprecipitation and mass spectrometry .....	27
2.7 Western blot quantification.....	29
Chapter 3: Results .....	30
3.1 hOLA1 depletion leads to upregulation of key anti-apoptotic proteins .....	30
3.2 hOLA1 depletion leads to decreased caspase activation in the MDA-MB231 cell line .....	41
3.3 hOLA1 depletion does not have considerable effects on the inhibition of cell death .....	45
3.4 Measurement of apoptosis in hOLA1-depleted cells.....	48
3.5 Co-immunoprecipitation and mass spectrometry to identify the protein(s) interacting with hOLA1 .....	51
Chapter 4: Discussion and future perspective .....	55
4.1 Discussion .....	55
4.2 Future perspectives .....	60
References .....	62

## List of Tables

Table 2.1: Antibodies used in this study.....	25
Table 3.1: Mass spectrometry data analysis of sample I (MW ~45 kDa).....	53
Table 3.2: Possible interacting partner of hOLA1.....	54

## List of Figures

Figure 1.1: Schematic representation of cap-dependent translation initiation.....	4
Figure 1.2: Schematic diagram of apoptotic pathway .....	15
Figure 1.3: hOLA1 as regulator of protein synthesis, possible mechanism suggested by Chen, H <i>et al</i> .....	20
Figure 3.1: Optimization of the concentration of si-hOLA1 for the depletion of hOLA1...	32
Figure 3.2: Optimization of si-hOLA1 transfection duration time for the effective depletion .....	33
Figure 3.3: hOLA1 depletion leads to diminished ISR.....	34
Figure 3.4 hOLA1 depletion leads to increased level of cIAP1 in MDA-MB231 and HEK-293T cell lines .....	36
Figure 3.5: hOLA1 depletion leads to increased level of cIAP2 in MDA-MB231 and HEK-293T cell lines .....	37
Figure 3.6: hOLA1 depletion does not have a considerable effect on the level of cFLIP <sub>L</sub> in MDA-MB231 and HEK-293T cell lines.....	39
Figure 3.7: hOLA1 depletion leads to increased levels of Bcl-xL in MDA-MB231 and HEK-293T cell lines .....	40
Figure 3.8: hOLA1 depletion does not have a considerable effect on the levels of XIAP .....	41
Figure 3.9: hOLA1 depletion leads to decreased caspase activation.....	45
Figure 3.11: hOLA1 depletion and apoptotic induction do not have considerable effects on the inhibition of cell death in MDA-MB231 cell line.....	47
Figure 3.11: hOLA1 depletion and apoptotic induction do not have considerable effects on the inhibition of cell death in HEK-293T cell line.....	48
Figure 3.12: hOLA1 depletion leads to decreased apoptosis.....	50
Figure 3.13: Co-immunoprecipitation to identify the protein(s) interacting with hOLA1 .....	53



## List of Abbreviations

ATF4 - Activating transcription factor-4  
Bcl-xL - B-cell lymphoma-extra large  
cFLIP<sub>L</sub> - Cellular FLICE-like inhibitory protein  
CHOP - C/EBP homologous protein  
cIAP1 - Cellular inhibitor of apoptosis 1  
cIAP2 - Cellular inhibitor of apoptosis 2  
CREP - Constitutive repressor of eIF2 $\alpha$  phosphorylation  
eIF2 - Eukaryotic initiation factor 2  
FADD - Fas-associated protein with death domain  
GADD34 - Growth arrest and DNA damage-inducible protein  
hOLA1 - Human obg like ATPase  
IAPs - Inhibitors of apoptosis  
PIC - Pre-initiation complex  
RIPA - Radioimmunoprecipitation assay  
TC - Ternary complex  
TGS - ThrRS, GTPase, SpoT  
TNF $\alpha$  - Tumor necrosis factor  $\alpha$   
TRADD - Tumor necrosis factor receptor type 1-associated DEATH domain protein  
TRAIL - TNF-related apoptosis-inducing ligand (TRAIL)  
XIAP - X- linked inhibitor of apoptosis protein

## **Chapter 1: Introduction**

### **1.1 Overview of eukaryotic gene expression**

The deoxyribonucleic acid (DNA) encodes protein molecules that carry out all essential functions of life.<sup>1</sup> The portion of a gene that encodes for a protein is called the coding region.<sup>2,3</sup> Transcription is the process of copying the genetic information stored in the DNA to a ribonucleic acid (RNA) molecule by RNA polymerase enzymes.<sup>1</sup> Once the primary transcripts are made they undergo post-transcriptional modifications such as 5' capping, polyadenylation, and splicing to form mature mRNA.<sup>4</sup> Capping is the addition of 7-methylguanosine (m<sup>7</sup>G) at the 5' end of the mRNA.<sup>4</sup> Polyadenylation involves the addition of around 250 adenine residues at the 3' end.<sup>4</sup> Splicing is the removal of the non-coding regions in the mRNA.<sup>4</sup> Once the mature mRNA is made, it is transported to the cytoplasm. In the cytoplasm, mature mRNA is translated into proteins using the translation machinery.<sup>5</sup> Translation is a fundamental cellular process which occurs in three different phases: initiation, elongation, and termination.<sup>5</sup>

#### **1.1.1 Cap-dependent translation initiation**

The initiation of translation involves several distinct steps leading to assembly of the 80S initiation complex.<sup>6</sup> Notably, initiation is highly regulated and a rate-limiting step of translation.<sup>6</sup> During initiation, the start codon is recognized and base-paired to initiator tRNA (Met-tRNA<sub>i</sub>) in the P site of 40S ribosomal subunit.<sup>5,7</sup> The initiation process involves three major steps: formation of the 43S pre-initiation complex, formation of the 48S pre-initiation complex, and formation of the 80S ribosome.<sup>6</sup> The first step of translation is the formation of ternary complex (TC; eIF2•GTP•Met-tRNA<sub>i</sub>) through the interaction of initiator tRNA with the eIF2 and guanosine triphosphate (GTP).<sup>8</sup> eIF2 is a GDP/GTP

binding protein complex consisting of three subunits; regulatory subunit- $\alpha$ , tRNA/mRNA binding subunit- $\beta$ , and guanine nucleotide binding subunit- $\gamma$ .<sup>5, 8</sup> Formation of the 43S initiation complex involves interaction of the TC with the 40S ribosomal subunit and other initiation factors, namely 1, 1A, and 3 (Figure 1.1).<sup>5, 9</sup> The 43S initiation complex is stabilized by eIF1 and eIF3.<sup>10, 11</sup> eIF1A promotes assembly of 43S preinitiation complex and ribosomal scanning along with eIF1 to recognize the start codon.<sup>10, 11</sup> The 5' m<sup>7</sup>G cap of cellular mRNA enhances the translation initiation through the interaction with cap-binding complex eIF4F.<sup>5, 7</sup> eIF4F is a heterotrimeric factor consisting of three initiation factors: RNA helicase eIF4A, cap-binding protein eIF4E, and molecular scaffolding protein eIF4G.<sup>5, 7</sup> The eIF4F complex binds to the 5' cap structure along with eIF4B, whereas Poly(A)-binding protein (PABP) binds to the poly-A tail at the 3' end of the mRNA.<sup>5, 7</sup> PABP has the ability to interact with eIF4G.<sup>5, 7</sup> This results in the circularization of mRNA.<sup>5, 7, 12</sup> Circularization of mRNA enhances the recruitment of 43S pre-initiation complex (PIC) to the mRNA and formation of the 48S initiation complex.<sup>5, 7, 12</sup> The RNA helicase eIF4A helps in unwinding 5' mRNA secondary structures and facilitates ribosomal scanning to identify the initiation codon.<sup>7, 9</sup> Once the initiator tRNA is delivered and base-paired with the start codon, eIF5 induces the hydrolysis of GTP by eIF2.<sup>9</sup> Subsequently, eIF5B facilitates the joining of the 40S and 60S ribosomal subunits.<sup>5, 13</sup> During this process eIF5B interacts with eIF1A on the C-terminus of eIF1A.<sup>14</sup>

After the 80S initiation complex has formed, the translation proceeds to the elongation phase, where polypeptide chain formation occurs.<sup>15</sup> During elongation, the elongation factor 1A (eEF1A) helps to recruit the next aminoacyl tRNA to the A site.<sup>15</sup> Peptide bond formation between the adjacent amino acids is catalyzed by the peptidyl transferase activity

of the ribosome.<sup>15, 16</sup> Elongation continues until the stop codon is encountered at the A site of the ribosome. Once the stop codon is recognized by eukaryotic releasing factor 1 (eRF1), eRF1 binds to eRF3 and GTP.<sup>15</sup> Subsequently eRF3 induces the hydrolysis of GTP to promote peptide chain release from the ribosomal complex. Subsequently, ATP-binding cassette subfamily E member1 (ABCE1) promotes ribosomal dissociation and releases the factors by an energy-dependent mechanism.<sup>15</sup> The released ribosomal subunits and eIFs are recycled and used in the next cycle of translation initiation.<sup>15</sup>

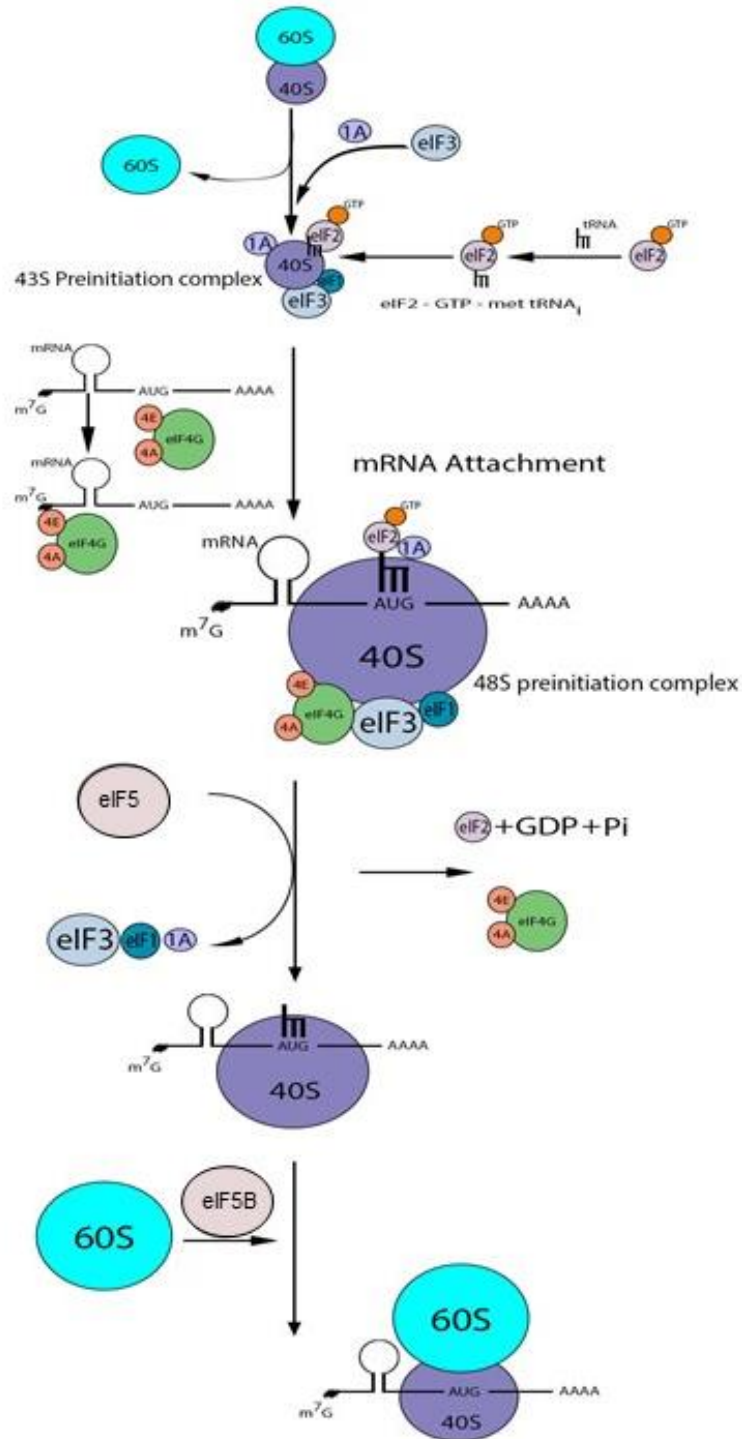


**Figure 1.1: Schematic representation of cap-dependent translation initiation:** The 40S subunit along with TC and other factors form the 43S pre-initiation complex (PIC). 43S is believed to scan 5' UTR of the mRNA to find a start codon in the right context. Following the Met-tRNA<sub>i</sub> delivery 48S pre-initiation complex is formed. Upon GTP hydrolysis and the release of eIFs, 60S ribosomal subunit unites with 40S subunit to form 80S ribosomal complex.

### 1.1.2 Cap-independent translation

The above described molecular mechanism of translation is also called the canonical or cap-dependent translation.<sup>6</sup> However, during stress, cap-dependent translation is inhibited by cleavage or modulation of several initiation factors.<sup>17</sup> During such stress conditions a subset of mRNAs continue to be translated *via* cap-independent translation initiation mechanisms.<sup>18</sup> Internal ribosome entry site (IRES)-mediated translation initiation is an example of cap-independent translation initiation.<sup>19,20</sup>

An IRES is a RNA element that has distinct secondary or tertiary structures and allows the translation of an mRNA through its interaction with few eIFs and *trans*-acting factors, without the involvement of the 5' cap structure.<sup>18</sup> IRES-mediated translation was first identified in the positive-stranded RNA poliovirus.<sup>19, 20</sup> Poliovirus infection leads to proteolytic cleavage of eIF4G, resulting in the loss of its interaction with eIF4E and eIF3, preventing the formation of the eIF4F complex, and thus inhibiting cap-dependent translation.<sup>21</sup> Although cap-dependent translation of cellular mRNA is inhibited, poliovirus RNA translation was observed to be stimulated during these conditions.<sup>21</sup> Poliovirus translation is conducted through a mechanism independent of eIF4F and the m<sup>7</sup>G cap structure.<sup>21</sup> This cap-binding complex-independent mechanism of translation initiation was later termed as IRES-mediated translation.<sup>21</sup> These viral IRESs were classified based on the RNA sequence and structural similarities and the factors required for translation initiation. For example, picornavirus IRESs classified into three types based on the different characteristics such as structure and the factors required for translation.<sup>22</sup> Type I and type II requires eIF4G and eIF4A.<sup>22</sup> Type III IRESs require eIF4G and only occurs in hepatitis A virus.<sup>22</sup>

Cellular IRESs were identified in stress response genes that encode for pro- and anti-apoptotic proteins: B cell lymphoma extra-large (Bcl-xL), apoptotic protease-activating factor 1 (APAF1), B-cell lymphoma 2 (Bcl-2), Bcl-2 associated athanogene1 (Bag-1), cellular inhibitor of apoptosis protein 1 (cIAP1), X-linked inhibitor of apoptosis protein (XIAP).<sup>23-26</sup> These pro-survival and death proteins are activated due to internal and external stress stimuli such as DNA damage, viral infection, hypoxia, nutrient deprivation and endoplasmic reticulum (ER) stress.<sup>24, 26</sup> During stress conditions several signaling pathways are activated to regulate protein synthesis in order to recover cellular homeostasis.<sup>26-28</sup>

### **1.1.3 Regulation of translation during the integrated stress response**

During stress condition, translation is regulated by activation or inhibition of initiation factors such as eIF4E homologous protein (4E-HP), eIF4E-binding proteins (4E-BPs) and eIF2.<sup>29, 30</sup> As mentioned below, these eIFs either regulate the recruitment of 40S subunit onto the mRNA or the recruitment of tRNA into the P site of 40S ribosomal subunit. Canonical translation initiation is extensively regulated by the 5'mRNA cap-binding protein eIF4E.<sup>31</sup> The cap recognition by eIF4E is hindered due to binding of 4E-HP to the cap structure.<sup>32, 33</sup> The 4E-HP protein could recognize cap structure, however, it lacks the ability to interact with eIF4G leading to the inhibition of protein synthesis.<sup>34</sup> In addition, the eIF4G-eIF4E interaction in the eIF4F complex is inhibited by 4E-BPs.<sup>32, 33</sup> 4E-BPs inhibit cap-dependent translation by competing with eIF4G for the shared binding site on eIF4E.<sup>33</sup> The interaction of 4E-BP with eIF4E is regulated by phosphorylation of 4E-BP. Hypo-phosphorylation of 4E-BP leads to its stronger binding with eIF4E, whereas hyper-phosphorylation of 4E-BP leads to weakening of the interaction with eIF4E.<sup>33</sup>

Phosphorylation of 4E-BP is regulated by a signaling pathway called mechanistic target of rapamycin (mTOR) pathway.<sup>35</sup>

One of the key regulatory mechanisms during stress is phosphorylation of the  $\alpha$  subunit of eIF2 complex.<sup>30, 36</sup> eIF2 mainly exists in either: GTP- bound or GDP- bound states.<sup>37</sup> During translation initiation, the inactive eIF2-GDP complex is recycled back to an active eIF2-GTP complex to regenerate the TC by a guanine nucleotide exchange factor called eIF2B.<sup>37</sup> During stress conditions, the  $\alpha$ -subunit of eIF2 is phosphorylated at serine 51 by one of the four eIF2 $\alpha$  kinases (discussed below).<sup>5</sup> Phosphorylation of eIF2 $\alpha$  enhances its affinity for eIF2B, leading to the sequestration of eIF2 by eIF2B. Inhibition of active eIF2-GTP regeneration results in decreased TC formation, thus inhibiting overall translation and activating stress response pathway such as integrated stress response (ISR).<sup>36-38</sup>

ISR is activated in response to various pathological and physiological conditions including both extrinsic and intrinsic stimuli. For example, nutrient deprivation, hypoxia, and ER stress can activate ISR.<sup>38-41</sup> The common convergence of ISR activation is the phosphorylation of the eIF2 $\alpha$  subunit.<sup>42</sup> Increased phosphorylation of eIF2 $\alpha$  leads to decreased cap-dependent translation while allowing the translation of selected mRNAs such as that encoding activating transcription factor 4 (ATF4) through 5' upstream open reading frames (5'uORF).<sup>43-45</sup> ATF4 translation is regulated through the involvement of two different uORFs: uORF1 and uORF2.<sup>46</sup> The uORF1 element contains three amino acids residues in length, whereas uORF2 contains 59 amino acids residues in length that overlaps the ATF4 coding region in an out-of-frame manner.<sup>47</sup> During normal conditions, ribosome translates uORF1 and resumes ribosomal scanning and re-initiation downstream of the uORF1 leading to the translation of uORF2 and bypassing start codon of ATF4.<sup>46</sup> During



stress, eIF2 $\alpha$  phosphorylation lowers the level of active eIF2-GTP complex which increases the time required for ribosomal scanning and re-initiation.<sup>47</sup> This leads to a higher probability of re-initiation at the ATF4 coding region thus translating ATF4.<sup>47</sup> ATF4 aids the cells to recover cellular homeostasis by reprogramming transcription of stress-related genes.<sup>38, 48, 49</sup>

On the other hand, some of the cellular stress response transcripts are translated through IRES-mediated translation during stress.<sup>50</sup> For example, XIAP is translated through IRES dependent mechanism during stress condition.<sup>50</sup> XIAP is known to be encoded by two distinct mRNAs: shorter and longer 5'UTR.<sup>51</sup> During normal conditions, XIAP is translated through the shorter 5'UTR.<sup>51</sup> However, during stress the longer IRES-containing 5' UTR helps in the translation of XIAP.<sup>51</sup> The combination of cap-dependent translation and IRES-mediated translation helps in the maintenance of XIAP level in response to cellular stress and adaptation.<sup>51</sup> eIF2 $\alpha$  phosphorylation and dephosphorylation help to recover cellular homeostasis during stressed conditions.<sup>38</sup> However, based on the severity and duration of the stress condition, eIF2 $\alpha$  may or may not get dephosphorylated. Hence, ISR plays a dual role in cellular survival, cell death, hence in the ultimate cell fate.<sup>38</sup>

## **1.2 Activation and termination of the ISR**

The eIF2 $\alpha$  can be phosphorylated by four distinct kinases: general control non-derepressible 2 (GCN2), heme-regulated eIF2 $\alpha$  kinase (HRI), double-stranded RNA dependent protein kinase (PKR) and PKR-like ER kinase (PERK).<sup>52-54</sup> These kinases are homologous in their catalytic domain and divergent in their regulatory domains.<sup>55</sup> Each eIF2 kinase is activated by a distinct type of stress. For example, PKR is activated by the infection of double-stranded RNA viruses.<sup>56-58</sup> The double-stranded RNA aids in the

dimerization of C-terminal domain of PKR and thus PKR gets activated.<sup>56-58</sup> Activated PKR phosphorylates eIF2 $\alpha$  which results into the inhibition of both viral and host protein synthesis. Notably, other types of stresses also activate PKR independent of dsRNA such as; oxidative stress, ER stress, and growth factor deprivation.<sup>58-60</sup> The eIF2 kinase PKR is also activated through caspase activity in the early stages of apoptosis (apoptosis is discussed in section 1.3).<sup>61</sup> Activation of caspase-8, -7 and -3 results in the cleavage of eIF2 kinase domain leads to activation of PKR.<sup>61</sup> This results in the phosphorylation of eIF2 $\alpha$  thus inhibiting translation.<sup>61</sup> eIF2 kinase GCN2 is a highly conserved from yeast to human and is activated due to amino acid deprivation.<sup>62</sup> During amino acid starvation, the levels of amino acetylated tRNA is decreased.<sup>62</sup> GCN2 senses the increased pool of uncharged tRNA and gets activated.<sup>62</sup> Also, UV light is reported to activate GCN2 through an unrevealed mechanism.<sup>63</sup> Like PKR activation, GCN2 activation leads to the phosphorylation of eIF2 $\alpha$  and attenuation of the global protein synthesis.<sup>54</sup>

PERK is localized in the endoplasmic reticulum (ER) and activated due to several conditions including the accumulation of unfolded proteins in the ER, changes in the calcium homeostasis, and the oxidative stress.<sup>64</sup> In normal conditions, the luminal domain of PERK is bound to glucose-regulated-protein 78 (GRP78).<sup>64</sup> During ER stress PERK is activated by two different mechanisms. It is activated through the dissociation of ER luminal bound GRP78 due to the accumulation of unfolded proteins in the ER lumen.<sup>65</sup> PERK is also activated by direct binding of an unfolded protein to its luminal domain.<sup>64</sup>

HRI is mostly expressed in erythroid cells and is involved in erythrocyte differentiation.<sup>66</sup> HRI kinase activity is regulated by heme through the formation of a disulfide bond between two monomers and preventing dimerization.<sup>66</sup> HRI can be activated by many stresses

independent of heme but with the support of heat shock proteins 70 and 90 (HSP70 and 90).<sup>67</sup> Importantly, eIF2 kinase family members have interconnections; they can act together for similar stresses.<sup>68</sup> For example, GCN2 and PERK can compensate for each other under a variety of stress conditions such as viral infection and ER stress.<sup>68, 69</sup>

As mentioned earlier, besides inhibition of global protein synthesis, phosphorylation of eIF2 $\alpha$  also induces the translation of transcriptional activator ATF4.<sup>70, 71</sup> Increased translation of ATF4 induces the expression of the transcription factor C/EBP homologous protein (CHOP) and ATF3.<sup>72, 73</sup> Together these protein factors activate ISR-CHOP signaling.<sup>74</sup> CHOP promotes apoptosis through upregulation of BH3-only pro-apoptotic Bcl-2 family members.<sup>75</sup> CHOP also regulates the expression of the pro-apoptotic protein death receptor 5 (DR5) protein and pro-apoptotic genes such as apoptotic protease activating protein 1 (APAF1).<sup>76</sup> Moreover, ATF4 itself can promote apoptosis through direct activation of the pro-apoptotic-protein Bcl-2.<sup>77</sup> Further, during ISR the inhibitors of apoptosis proteins cIAP1, cIAP2, Livin, Survivin, NAIP, and XIAP are downregulated upon chronic PERK signalling.<sup>78</sup>

In addition to eIF2 $\alpha$  kinases, phosphatases play a critical role in executing ISR.<sup>79</sup> The eIF2 $\alpha$  dephosphorylation is a key point for the termination of ISR to recover global protein synthesis and cellular homeostasis.<sup>2, 79</sup> The eIF2 $\alpha$  dephosphorylation is implemented by the phosphatase activity of the constitutive repressor of eIF2 $\alpha$  phosphorylation (CReP), and growth arrest and DNA damage-inducible protein (GADD34).<sup>70, 80</sup> CReP helps unstressed cells to maintain translational homeostasis by maintaining a low level of eIF2 $\alpha$  phosphorylation through its constitutive function as eIF2 $\alpha$  phosphatase.<sup>80</sup> GADD34 expression is induced in later stages of ISR to dephosphorylate eIF2 $\alpha$ .<sup>81</sup> GADD34 helps in

the dephosphorylation of eIF2 $\alpha$  by interacting with protein phosphatase 1 (PP1).<sup>71</sup> The GADD34-PP1 complex acts as a negative feedback loop during ISR and helps the cells to recover homeostasis.<sup>71</sup> Furthermore, dephosphorylation of eIF2 $\alpha$  by GADD34 also helps the cells to allow the translation of the stress-responsive mRNAs such as HSP70.<sup>82</sup> If the cellular homeostasis is failed by phosphatase activity of GADD34, that can facilitate cell death by inducing death inducing-proteins such as DR5 and Bcl-2 family pro-apoptotic proteins.<sup>83, 84</sup>

On the other hand, early/mild ISR can also promote cell survival through negative regulation of apoptosis.<sup>85</sup> PERK-mediated ISR activation resulted in increased levels of cIAP1 and cIAP2 in both cancer and non-cancer cell lines and promote cellular survival.<sup>86</sup> As mentioned earlier, the consequences of eIF2 $\alpha$  phosphorylation differ based on the type of the stress condition such as chronic or acute and downstream effect of ATF4 translation and other factors.<sup>2, 54</sup>

### **1.3 Apoptosis or programmed cell death**

The balance between cell survival and cell death pathways is important for maintaining cellular homeostasis.<sup>87</sup> Cell death can be executed by programmed mechanisms such as apoptosis and necroptosis.<sup>87</sup> Apoptosis is an energy requiring mechanism that occurs normally to maintain tissue/organ homeostasis during development and aging.<sup>88</sup> Additionally, a wide variety of stress stimuli such as DNA damage and viral infection induce apoptosis.<sup>89</sup> Apoptosis can be characterized by morphological changes such as cell shrinkage, nuclear condensation, membrane blebbing or biochemical features such as caspase (cysteine-aspartic proteases) cleavage and DNA fragmentation.<sup>87</sup> Apoptosis is mediated by intracellular enzymes called caspases.<sup>90</sup> Fourteen different caspases have been

found in humans so far, out of which caspases- 2, 3, 6, 7, 8, 9, and 10 are known to play crucial roles in apoptosis.<sup>90</sup> These enzymes are expressed as inactive proenzymes.<sup>91</sup> Caspases consist of prodomain p20 large subunit and a p10 small subunit.<sup>92</sup> Activation of these proenzymes requires a proteolytic cleavage between small and large subunits that results in heterodimer active caspases.<sup>92</sup> Based on the length of their pro-domain, caspases are classified into two groups: initiator caspases (caspases 8, 9, 10) and executioner caspases (caspases 3, 6, 7).<sup>91</sup> Initiator caspases contain a long pro-domain that comprises a protein-protein interacting domain, caspase recruiter domain (CARD) and death effector domain (DED). Upstream adaptor proteins such as fas-associated protein with death domain (FADD) and tumor necrosis factor receptor type 1-associated DEATH domain protein (TRADD) interact with caspases through CARD and DED domains.<sup>91, 92</sup> In contrast, effector caspases containing a short pro-domain are classically activated by upstream initiator caspases.<sup>91, 92</sup> The activation of executioner caspases leads to subsequent cleavage of multiple cellular proteins and execution of cell death.<sup>91, 92</sup> Apoptosis can be triggered by many stimuli and is executed through two major pathways namely the extrinsic pathway, and intrinsic (mitochondrial) pathway.<sup>93</sup>

### **1.3.1 Mitochondrial or intrinsic pathway**

The mitochondrion is an important cellular organelle that is critical for energy production and deciding cell fate.<sup>94</sup> The intrinsic apoptotic pathway is activated through various intracellular signals such as DNA damage or nutritional deprivation leading to the mitochondrial outer membrane permeabilization (MOMP).<sup>95</sup> In normal condition, the Bcl-2 family protein Bax is found in the cytosol as monomers or loosely attached to the outer membrane of the mitochondria.<sup>96</sup> Another member of Bcl-2 family, Bak, is anchored into

the outer mitochondrial membrane in its monomeric form.<sup>97</sup> During apoptosis, Bax is localized to the mitochondrial outer membrane.<sup>96</sup> Bak and Bax oligomerize and form pores on the outer mitochondrial membrane.<sup>97</sup> This leads to release of mitochondrial proteins such as cytochrome c (cyt c), endonuclease D (EndoG), HtrA2/Omi, apoptosis-inducing factor (AIF), and second mitochondria-derived activator of caspase/direct IAP binding protein (Smac/DIABLO) into the cytosol.<sup>95, 97, 98</sup> Cytochrome c (cyt c) forms a complex in the cytoplasm with adaptor protein APAF1.<sup>99</sup> Subsequently, the APAF1-cyt c complex forms a heptameric structure through oligomerization.<sup>99</sup> Heptameric structure formation of APAF1-cyt c complex permits the interaction of procaspase-9 with APAF1.<sup>99</sup> This interaction leads to the activation of Caspase-9. When caspase-9 is activated, it activates effector caspases (3 and 7) to execute cell death (Figure 1.3).<sup>100</sup> On the other hand, mitochondrial proteins Smac/DIABLO and HtrA2/Omi promote caspase activation by blocking IAP-mediated caspase inhibition.<sup>101, 102</sup>

### **1.3.2 Extrinsic pathway**

The extrinsic pathway is initiated through the interaction of the death receptors present on the cell surface with their ligands.<sup>103</sup> The extracellular receptor ligands, such as tumor necrosis factor  $\alpha$  (TNF $\alpha$ ), TNF-related apoptosis-inducing ligand (TRAIL)/Apo2L, and Fas ligand (FasL)/CD95L bind to their corresponding membrane receptors TNFR, DR4/DR5, and Fas/CD95 respectively.<sup>104</sup> Death receptor contains a specific amino acid sequence termed death domain (DD).<sup>104</sup> Death domain is crucial for the transduction of apoptotic stress stimuli from extracellular receptors. Once the receptors and the ligand bind together, a cytoplasmic adapter protein is recruited onto the receptor-ligand complex through DD.<sup>104</sup> The pro-apoptotic ligand, receptor, pro-caspases and DD recruitment lead to the formation

of a new complex called death-induced signaling complex (DISC) and subsequent activation of initiator caspases.<sup>103, 104</sup> Activation of initiator caspases-8 and -10 leads to the cleavage of executioner caspases such as caspases-3 and -7 (Figure 1.3).<sup>104</sup> Notably, caspase-8 can also cleave BH3-only pro-apoptotic protein Bid to form truncated Bid (t-Bid) leading to MOMP and subsequent activation of the intrinsic apoptosis pathway.<sup>105</sup>

As mentioned below, TRAIL and TNF $\alpha$  execute apoptosis through distinct components of the extrinsic apoptosis pathway. The major differences between TRAIL and TNF $\alpha$  induced apoptosis are the receptors and cytosolic adaptor proteins.<sup>106</sup> TRAIL facilitates FADD recruitment onto the receptor upon binding to the appropriate receptors (DR4 or DR5) leading to the activation of caspase-8 and caspase-10.<sup>107</sup> On the other hand, TNF- $\alpha$  induces TNFR signaling leading to both apoptotic and non-apoptotic responses through the formation of two different complexes: complex I and complex II.<sup>107</sup> The complex I consists of TRADD, TRAF2, cIAPs, and receptor interacting protein-1 (RIP-1) to the activation of nuclear factor kappa-light-chain-enhancer of activated B cells (NF- $\kappa$ B) in order to promote cellular survival.<sup>106</sup> When complex I dissociates from RIP I and associate with procaspase-8 and FADD results in the formation of complex II in the cytosol. Complex II formation leads to the activation of the apoptotic pathway.<sup>106, 107</sup>

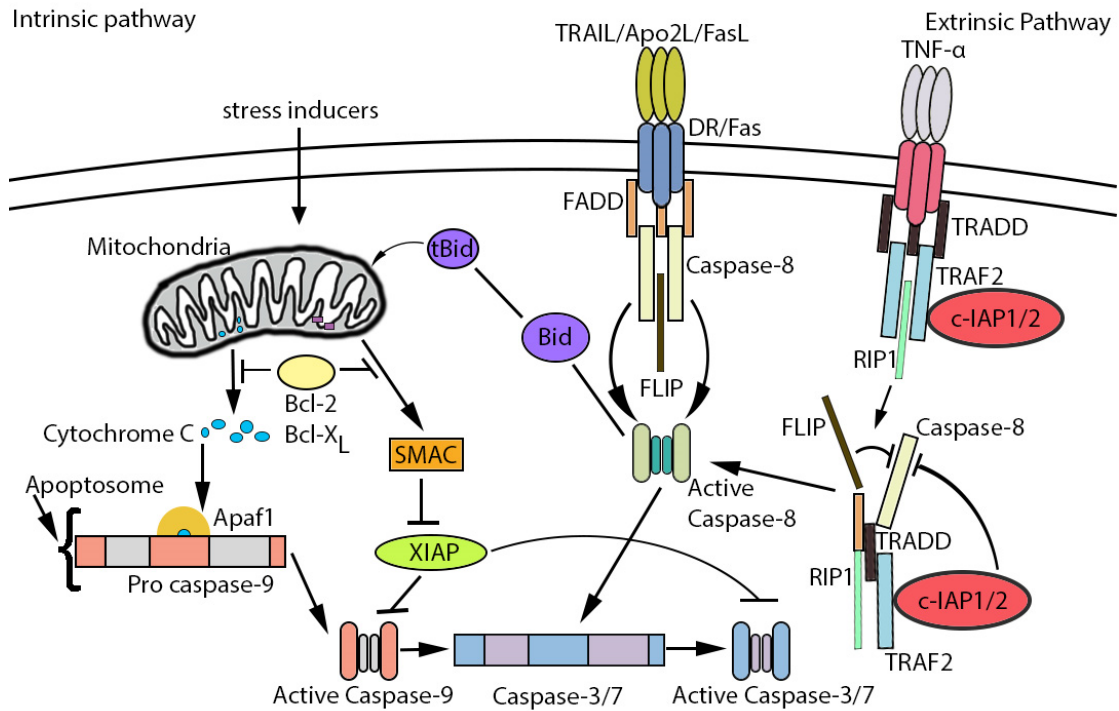


**Figure 1.3: Schematic diagram of the apoptotic pathways. Intrinsic pathway:** Intrinsic apoptosis is triggered by genotoxic stress. The major event is the recruitment of Bax and Bak on the outer mitochondrial membrane that causes the release of cytochrome c. Cytochrome C binds to APAF1 to form the apoptosome complex. The apoptosome activates caspase-9 that leads to the activation of caspase 3/7 and eventually execute apoptosis. **Extrinsic pathway:** extrinsic apoptosis is triggered by external stimuli by binding of ligands (FasL, APO-2L, TRAIL, TNF $\alpha$ ) to appropriate receptors (Fas, DR4, DR5, TNF-R1). Subsequent activation of procaspases-8 and -10 by recruiting adaptor protein FADD leads to the activation of caspase-8 or -10. This leads to the activation of executioner caspase-3, -6, -7 to mediate apoptosis. Also, there is a cross-talk between the intrinsic and extrinsic pathways. Caspase-8 can cleave Bid to form tBid leading to activation of the intrinsic apoptotic pathway.

### 1.3.3 Regulation of apoptosis

Apoptosis is regulated by anti- and pro-apoptotic proteins.<sup>108</sup> Proteins corresponding to the negative regulation of apoptosis are called anti-apoptotic proteins.<sup>93, 108, 109</sup> One of the main groups of anti-apoptotic proteins are the inhibitors of apoptosis proteins (IAPs), originally identified in the Baculovirus for their ability to regulate the enzymatic activity of caspases.<sup>108-111</sup> Later, IAPs were identified in mammals as well as fruit flies.<sup>111</sup> There are eight different human analogs from the IAP families: X-linked inhibitor of apoptosis



(XIAP), Apollon/Bruce, cellular inhibitor of apoptosis protein1 (cIAP1), cellular inhibitor of apoptosis2 (cIAP2), Survivin, IAP-like protein 2 (ILP2), melanoma IAP (ML-IAP/Livin) and neuronal apoptosis inhibitory protein (NAIP).<sup>112</sup> The important hallmark of IAP is that they all have at least one baculoviral IAP repeat (BIR) domain.<sup>112</sup> With the exception of Survivin, IAPs have one or more functional domains either a really interesting new gene (RING) domain, or a caspase recruitment domain (CARD), or both.<sup>113</sup> The RING domain possesses E3 ligase activity allowing the self-regulation of IAP by proteasomal degradation, whereas the CARD domain is involved in protein-protein interaction.<sup>114</sup> Caspases are inhibited by BIR2 and BIR3 domains.<sup>91</sup> The BIR2 domain specifically targets caspase-3 and caspase-7 whereas BIR3 domain targets caspase-9 and degraded by ubiquitylation.<sup>91</sup>

XIAP is crucial among IAPs that suppress both extrinsic and intrinsic apoptotic pathways.<sup>115</sup> It contains BIR2 and BIR3 domains to inhibit an upstream caspase (caspase-9) and downstream caspases (caspase-3 and 7).<sup>116</sup> The BIR2 domain interacts with the N-terminal small subunit of caspase-3 and caspase-7 to prevent substrate binding. On the other hand, the BIR3 domain binds to the IAP binding motif of caspase-9.<sup>115</sup> Also, XIAP can inhibit apoptosis *via* proteolytic degradation by E3 ligase activity of its RING domain.<sup>116</sup> cIAP1 and cIAP2 are homologs that inhibit the extrinsic pathway through their interactions with TRAF1 and TRAF2.<sup>111, 117</sup> cIAP1 and cIAP2 contain three BIR domains, a CARD domain, and a RING domain.<sup>117</sup> In addition, cIAP1 and cIAP2 inhibit apoptosis by activating the NF- $\kappa$ B pathway.<sup>117</sup> Caspase inhibition by IAPs are antagonized by Smac/DIABLO family mediated poly-ubiquitylation.<sup>118</sup> Although Survivin contains one

BIR domain, it does not inhibit caspases, whereas Livin contains one BIR domain that inhibits caspase-3 and 9.<sup>112, 113, 119</sup>

An additional group of anti-apoptotic proteins are the Bcl-2 family anti-apoptotic members (Bcl-2, Bcl-X, and Bcl-xL) that are associated with the outer mitochondrial membrane and prevent apoptosis.<sup>120</sup> The Bcl-2 family has pro-apoptotic members as well, such as Bak, Bid and Bax that facilitate the release of cytochrome c into the cytosol and thus activate the intrinsic apoptotic pathway.<sup>120, 121</sup>

The anti-apoptotic protein of extrinsic apoptotic pathway is cellular-FADD-like IL-1 $\beta$ -converting enzyme-inhibitory protein (cFLIP).<sup>122</sup> There are several splice variants of cFLIP. However, only three are expressed at the protein level: c-FLIP long (c-FLIP<sub>L</sub>), c-FLIP short (c-FLIP<sub>S</sub>) and a short variant c-FLIP<sub>R</sub>.<sup>122</sup> All three isoforms of cFLIP can be recruited to the DISC complex through death effector domain (DED, a subclass of DD).<sup>122</sup> cFLIP inhibit caspase-8 activation at the DISC by competing with caspase-8 to bind to FADD.<sup>123</sup> Dysregulation of anti- and pro-apoptotic proteins have been reported in many type of cancers: pancreatic cancer, melanoma and lymphoma.<sup>124</sup> This underlines the importance of studying detailed mechanisms of apoptotic regulators.<sup>112</sup>

#### **1.4 Role of translational control in cancer**

Dysregulation of gene expression at the translation level has been implicated in oncogenesis and cancer progression.<sup>125</sup> As mentioned earlier, translation is mostly regulated at the initiation stage.<sup>126</sup> Overexpression of the initiation factors such as eIF3, eIF4G, eIF5A is observed in many types of malignancies.<sup>25</sup> Also, some initiation factors can act as both tumor inducer and as tumor suppressors.<sup>25</sup> For example, the h subunit of eIF3-complex is overexpressed in breast cancer whereas the f subunit of the eIF3-complex

is observed to be decreased in melanoma and pancreatic cancer.<sup>127, 128</sup> The crucial regulatory factors of cap-dependent translation, eIF4E, and eIF4G are overexpressed in breast cancer and lung carcinoma.<sup>129, 130</sup> During the conditions when global protein synthesis is dysregulated by changes in the level of initiation factors, translation could rely on the cap-independent mechanism.<sup>6, 18</sup> For example, during stress, genes that promote survival and tumor growth such as Bcl-2, VEGFA are translated *via* IRES-mediated mechanisms.<sup>25</sup> Besides initiation factors other factors like *trans*-acting factors, miRNAs and nucleotide-binding proteins also known to regulate protein synthesis.<sup>131, 132</sup>

### **1.5 Human obg like ATPase1**

Human obg like ATPase1 (hOLA1) is a nucleotide-binding protein that has numerous crucial roles in various cellular processes like translation, cell motility, cell division and cytoskeleton organization.<sup>133, 134</sup> hOLA1 belongs to the phosphate-binding loop nucleotide triphosphatase (P-loop NTPase) group.<sup>133</sup> The P-loop GTPase is a subclass of nucleotide-binding protein that facilitates the hydrolysis of GTP to regulate fundamental cellular processes such as cell division, signal transduction and translation.<sup>133</sup> P-loop GTPases are further classified into two major groups based on structural features and conserved sequences: translation factor related class (TRAFAC) and signal recognition particle.<sup>133</sup>

P-loop GTPases contain a common core G-domain with five conserved motifs.<sup>133</sup> These motifs are responsible for several functions such as GTP binding, GTP positioning, guanine nucleotide recognition, and magnesium ( $Mg^{2+}$ ) coordination.<sup>133</sup> These properties of the G domain provide conformational flexibility to the protein during nucleotide hydrolysis.<sup>133</sup> Additionally, the central G domain of OLA1 is flanked on either side by a coiled-coil domain and a TGS (ThrRS, GTPase, SpoT) domain.<sup>133</sup> P-loop GTPases are further

classified into four families: protein secretion factors, Era-related GTPases, Elongation factors (EF-G, EF-Tu, Lep A, and IF2) and Obg-related family (Obg and YchF).<sup>133</sup>

hOLA1 is an ATP and GTP binding protein that belongs to obg1 family of P-loop GTPase.<sup>134</sup> It was first identified and characterized in 2007.<sup>134</sup> hOLA1 is reported to have a higher affinity for ATP compared to GTP.<sup>134</sup> Therefore, hOLA1 was named as human Obg like ATPase1.<sup>134</sup> hOLA1 is abnormally expressed in different type of cancers, suggesting the importance of studying the role of hOLA1 in stress conditions.<sup>135</sup> Indeed, hOLA1 is known to play numerous roles during stress conditions as discussed below.<sup>135-137</sup> hOLA1 is a negative regulator of antioxidant response.<sup>135</sup> hOLA1 prevents ubiquitylation-mediated degradation of HSP70.<sup>137</sup> Also, hOLA1 plays an important role in centrosome regulation through the interaction with breast cancer associated gene1 (BRCA1) and  $\gamma$ -tubulin in breast cancer cell lines.<sup>138, 139</sup> In addition, hOLA1 was also referred to as the DNA damage-regulated overexpressed in cancer 45 (DOC45) because it is implicated in DNA damage response.<sup>140</sup> hOLA1 is a protein synthesis, cell cycle, and ISR regulator.<sup>136</sup> The next two sections describe how hOLA1 regulates protein synthesis, ISR, and cell cycle.

### **1.5.1 hOLA1 as a regulator of protein synthesis and ISR.**

hOLA1 is reported to inhibit protein synthesis and ISR by inhibiting TC formation.<sup>136</sup> hOLA1 is known to suppress protein synthesis by limiting the formation of TC.<sup>136</sup> Importantly, hOLA1 is known to interact with eIF2.<sup>136</sup> In addition, Chen, H *et al.* reported that hOLA1 depletion leads to greater TC level and diminished ISR.<sup>136</sup> Moreover, Chen, H *et al.* also reported that hOLA1 depletion leads to increased cellular survival and a diminished CHOP level.<sup>136</sup> Further, *in vivo* analysis revealed that hOLA1 depletion leads to deficient ISR, tumor growth and metastasis.<sup>136</sup> Chen, H *et al.* suggested a mechanism

for the role of hOLA1 in regulating protein synthesis, they believed that hOLA1 facilitates the hydrolysis of eIF2-bound to GTP leading to the formation of an inactive eIF2-GDP complex, which is unable to bind to Met-tRNA<sub>i</sub>, thus inhibiting TC formation (Figure 1.3).

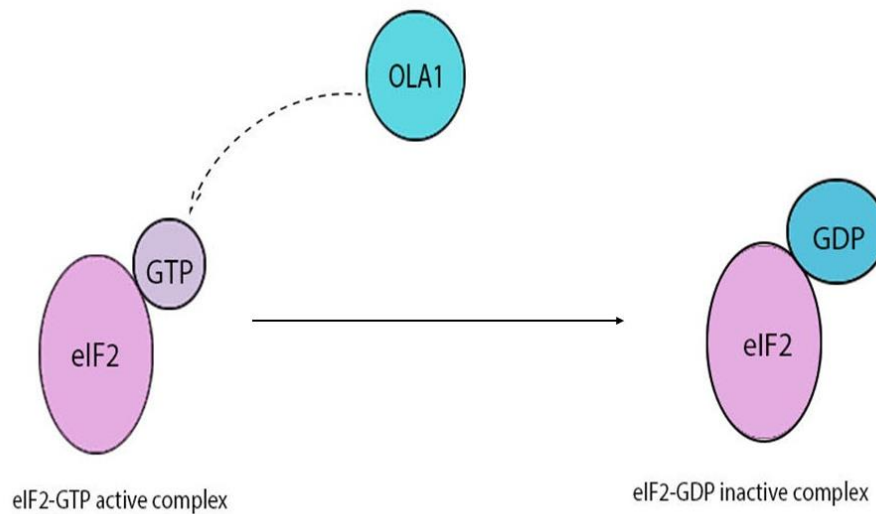


**Figure 1.3: hOLA1 as regulator of protein synthesis, possible mechanism suggested by Chen, H *et al.*** Chen, H *et al.* suggested a possible mechanism for the regulation of protein synthesis by hOLA1.<sup>136</sup> hOLA1 is known to interact with eIF2 and thus possibly inhibiting TC formation, therefore Chen, H *et al.* suggested that hOLA1 inhibit TC formation by facilitating the hydrolysis of GTP bound to eIF2 into eIF2-GDP, thus inhibiting global protein synthesis.<sup>136</sup>

### 1.5.2 hOLA1 as a cell cycle regulator

The cell cycle is a key cellular function that leads to the cell division.<sup>141</sup> One of the main cause of cancer is dysregulation of the cell cycle.<sup>142, 143</sup> Cyclins and cyclin-dependent kinases (CDKs) are essential enzymes for the transition of the cell cycle from one phase to the next phase in mammalian cells.<sup>142</sup> The G1 to S phase transition requires cyclins D and E, the G2 to M transition requires the formation of the cyclin B-CDK1 complex by dephosphorylation of CDK1.<sup>142</sup> This phase transition is inhibited by cyclin-dependent kinase inhibitors: p21, p27, and p53.<sup>142</sup> hOLA1 is known to regulate the cell cycle by

suppressing CDK2 inhibitor p21. It was demonstrated that p21 is translationally regulated by hOLA1.<sup>143</sup>

## **1.6 Aim of the project**

As mentioned earlier hOLA1 suppresses protein synthesis by inhibiting TC formation.<sup>136</sup> Moreover, hOLA1 is known to interact with eIF2 and depletion of hOLA1 leads to diminished ISR and enhanced cellular survival.<sup>136</sup> Enhanced cellular survival could be the result of increased cell proliferation or decreased apoptosis. Depending on the type of the stress condition ISR plays an important role in deciding cell fate by regulating anti- and pro-apoptotic proteins.<sup>50</sup> *Therefore, I hypothesize that increased survival in hOLA1-depleted cells is due to the upregulation of anti-apoptotic proteins and inhibition of apoptosis.* The main objectives of this project are as follows.

### **1. To elucidate the role of hOLA1 in apoptosis and ISR.**

The role of hOLA1 in apoptosis was assessed using knockdown studies and Western blotting. Western blots were used to assess the levels of anti-apoptotic proteins, cleaved caspase, and PARP cleavage. The viability assay (alamarBlue™ assay) was used to measure cell viability. Propidium iodide (PI) staining and flow cytometry were used to quantify apoptosis.

### **2. To identify the proteins interacting with hOLA1.**

As mentioned earlier, hOLA1 is known to regulate protein synthesis by inhibiting ternary complex formation.<sup>136</sup> In addition, hOLA1 is reported to interact with eIF2.<sup>136</sup> However, it is not clear as to how hOLA1 regulates protein synthesis. Therefore, I wanted to assess if there are additional proteins that regulate the interaction of hOLA1 with eIF2. To this end, I performed co-immunoprecipitation and mass spectrometry to identify additional protein(s) interacting with hOLA1.

## **Chapter 2: Materials and methods**

### **2.1 Cell lines**

The human breast cancer cell line: MDA-MB231 was obtained from the children's hospital of eastern Ontario (CHEO). The human embryonic kidney cell line HEK-293T was purchased from American type culture collection (ATCC). Cells were cultured using Dulbecco's Modified Eagle's medium (DMEM) with 10% (v/v) Fetal Bovine Serum (FBS, Gibco), 50 U/ml Penicillin, 50 µg/ml Streptomycin, and 200 µM L-Glutamine. The cells were cultured in 10 cm Petri dishes under conditions of 5% CO<sub>2</sub> and 37 °C. Trypsin (Final concentration: 0.25% (wt/v) Trypsin, 1.45 mM NaCl, 0.5 mM EDTA in PBS) was used for detaching cells for sub-culturing.

### **2.2 Transfection**

For hOLA1 knockdown, Human OLA1 cDNA (NM\_013341.3) specific siRNA (SASI\_Hs01\_00244684) and the control siRNA (MISSION siRNA Universal Negative Control #1 SIC001) were obtained from Sigma-Aldrich. Lipofectamine® RNAiMAX transfection reagent (Thermofisher Scientific) was used to deliver the siRNA to the cells; the transfection mix was prepared according to the manufacturer's instructions. 250 µl of Opti-MEM, 6 µl of Lipofectamine® RNAiMAX and 50 nM (final concentration) of siRNA were added and incubated for 20 minutes at 37 °C in the incubator. The cells were stained with 0.4% (wt/v) Trypan Blue (Thermofisher, Catalog number: 15250061) and counted using hemocytometer, MDA-MB231 cells ( $1.5 \times 10^5$ ) and HEK-293T cells ( $1.0 \times 10^5$ ) were seeded in the 6-well plates. Following cell seeding, transfection mix was added, and the plate incubated at 37 °C in an incubator with the 5% CO<sub>2</sub> for 96 hours.



### **2.3 Western blotting**

Cells were harvested in RIPA (Radio Immuno Precipitation Assay) lysis buffer containing 50 mM Tris-HCl pH 7.4, 1mM EDTA, 15mM NaCl, 1% (v/v) NP40, 0.5% (wt/v) deoxycholic acid, 0.05% (wt/v) SDS, protease inhibitors (Final concentration: 0.01 µg/µl Leupeptin, 0.005 µg/µl PMSF, 0.013 µg/µl Aprotinin, 0.001 µg/µl Pepstatin A) and phosphatase inhibitors (0.209 µg/µl NaF and 3.689 µg/µl NaV). The whole cell lysate was centrifuged using a Sorvall™ ST 8 Small Benchtop Centrifuge at 10,000g for 15 minutes to remove the cell debris. The supernatant was collected, and the protein concentration was quantified using Quick Start™ Bradford reagent as per manufacturer's protocol (Bio-Rad, Catalog No:5000201). 10 µg of proteins were separated on 12% SDS-PAGE. The proteins were then transferred onto a nitrocellulose membrane. The membrane was blocked with 10% (wt/v) skim milk in PBST (137 mM NaCl, 2.7 mM KCl, 10 mM Na<sub>2</sub>HPO<sub>4</sub>, and 1.8 mM KH<sub>2</sub>PO<sub>4</sub>, 0.02% (v/v) Tween) for one hour at room temperature. Following blocking, the membrane was incubated with 10 mL of primary antibody (Diluted in 0.02% PBST with 1% skimmed milk as per manufacturer's instruction, Table 2.1) overnight at 4°C. The next day, blots were washed with PBST (0.02% (v/v) tween) two times and once with PBS (137 mM NaCl, 2.7 mM KCl, 10 mM Na<sub>2</sub>HPO<sub>4</sub>, and 1.8 mM KH<sub>2</sub>PO<sub>4</sub>). Subsequently, the blots were incubated with 10 mL of horseradish peroxidase (HRP) conjugated secondary antibody (1:3000 dilution in 1% skimmed milk in PBST) for one hour at room temperature. Subsequently, the bands were visualized using enhanced chemiluminescence (ECL) substrate (Thermofisher Scientific, catalog number: 32106) in Amersham imager 600.

**Table 2.1:** Antibodies used in this study

<b>Antibody</b>	<b>Dilution</b>	<b>Catalog No</b>	<b>Source</b>
Anti-hOLA1 antibody	1:1000	HPA035790	Sigma
Anti-GTPBP9 antibody	1:1000	ab51077	Abcam
Anti-cIAP1 antibody	1:1000	ab2399	Abcam
Anti-cIAP2 antibody	1:1000	ab23423	Abcam
Anti-XIAP antibody	1:1000	ab21278	Abcam
Anti-FLIP antibody	1:1000	ab8421	Abcam
Anti- Bcl-xL antibody	1:1000	ab31396	Abcam
Anti-ATF-4 antibody	1:1000	ab1371	Abcam
Anti-CHOP antibody	1:1000	D46F1	Cell signalling Technology (CST)
Anti-rabbit IgG, HRP-linked antibody	1:3000	7074S	CST
Anti-Caspase-8 antibody	1:1000	9496S	CST
Anti-Caspase-7 antibody	1:1000	12827S	
Anti-Caspase-9 antibody	1:1000	9502S	
Anti-Caspase-3 antibody	1:1000	9662S	
Anti-Cleaved PARP antibody	1:1000	5625S	
Anti-GAPDH antibody	1:10,000	ab9485	Abcam

#### **2.4 alamarBlue™ assay**

MDA-MB231 and HEK-293T cells were transfected with siRNA in a 96-well plate, at 24 hours post-transfection, apoptotic inducers were added: doxorubicin (10 nM), TRAIL (100 ng/mL), TNF $\alpha$  (100 ng/mL). Following 72 hours of apoptotic inducers treatment, 10  $\mu$ l of alamarBlue™ dye (Resazurin sodium salt in water, final concentration-3 mg/mL, obtained from Sigma) was added. Subsequently, cells were incubated for 16 hours. At the end of 16 hours, the fluorescence absorbance at 600 nm was measured.

#### **2.5 Propidium iodide (PI) staining and flow cytometry**

MDA-MB231 cells ( $1.5 \times 10^5$ ) were seeded and transfected with 50 nM control siRNA and 50 nM si-hOLA1. After 92 hours of transfection, cells were treated with DMSO and 100 ng/mL TRAIL. Cells were trypsinized 96 hours post-transfection (after 4-hours of compound treatment), washed with PBS (137 mM, NaCl, 2.7 mM KCl, 10 mM Na<sub>2</sub>HPO<sub>4</sub>, and 1.8 mM KH<sub>2</sub>PO<sub>4</sub>). Cells were then re-suspended in 40  $\mu$ l PBS. Subsequently, 400  $\mu$ l of 70% (v/v) cold ethanol was added along the sides of the tube and mixed well. This step was repeated to make the total volume of 1 mL and kept at 4°C overnight. The next day, the cells were centrifuged using a Sorvall™ ST 8 Small Benchtop Centrifuge at 4,000g, 4°C for 5 minutes. The pellet was washed with PBS and centrifuged using a Sorvall™ ST 8 Small Benchtop at 4,000g, 4°C for 5 minutes, then the pellet was re-suspended in 30  $\mu$ l PBS containing 2  $\mu$ l of 10 mg/mL RNase. The re-suspended pellet was then incubated at 37°C for 4 hours. Following the incubation, the PI (PI staining solution obtained from Sigma, final concentration 1  $\mu$ g/ $\mu$ l of PI with 2mM MgCl<sub>2</sub> in 1 $\times$ PBS) solution was added and incubated at 37°C for 15-30 minutes. Subsequently, cells were submitted for flow cytometry analysis (flow cytometry facility, University of Alberta). Samples were acquired on an Attune NxT cytometer. Single cells (100,000) were acquired from each sample, based

on gating forward scatter (FSC-A vs SSC-A) versus side scatter (cells) and PI-A vs PI-W (single cells). All samples were analyzed using FlowJo v10 Cell Cycle Platform (Watson (Pragmatic) model).

## **2.6 Immunoprecipitation and mass spectrometry**

MDA-MB231 cells were grown in a 10 cm dish for immunoprecipitation. Subsequently, cells were lysed when they reached 80% confluency using 1 mL RIPA lysis buffer (details are given in 2.1 section). The whole cell lysate was centrifuged using a Sorvall™ ST 8 Small Benchtop Centrifuge at 4°C, 10,000g for 15 minutes. The beads for the protein pull-down were obtained from ThermoFisher Scientific (Dynabeads™ protein G for immunoprecipitation, catalog number: 10003D). First, the beads were coated with hOLA1 antibody (Sigma, catalog number: HPA035790) by incubating 40 µl beads with 1 µg antibody overnight at 4°C in a Digital Tube Revolver (Thermo Scientific). Next, the cell lysate was incubated with anti-hOLA1 antibody-coated beads for 3 hours at 4°C in a rocker. The beads were washed with PBS, and the proteins were then eluted using 60 µl 2x Laemmli Sample Buffer (Bio-Rad, catalog number: #1610737). Next, a portion of the sample was assessed by Western blot technique. The membrane was probed with anti-hOLA1 antibody to verify the pull-down, and anti-eIF2 $\alpha$  antibody (Cell Signalling Technology, catalog number: #9722). Subsequently, another portion of the sample was analyzed on SDS-PAGE and stained with Coomassie stain for mass spectrometry analysis. Protein bands were then excised from the gel and de-stained. Subsequently, the gel plugs were washed with 150 µl water and incubated in a thermoshaker at 1,050 rpm for 5 minutes. The gel plugs and water were centrifuged at max speed in a mini-centrifuge for 5 minutes and the solution was removed using pipette. Then, the gel plugs were washed with 150 µl

acetonitrile by incubating in a thermoshaker at 1050 rpm for 5 minutes. Subsequently, the gel plugs were incubated with 100  $\mu$ l of 10 mM dichlorodiphenyltrichloroethane (DDT) at 56°C for 50 minutes. Next, the gel fragments were washed with acetonitrile as mentioned above. Then, the gel fragments were incubated with iodoacetamide for 20 minutes in a thermoshaker at 26°C and 1,050 rpm. Subsequently, the gel fragment was incubated with 150  $\mu$ L of 100 mM  $\text{NH}_4\text{HCO}_3$  and incubated at 26°C in a thermoshaker at 1,050 rpm for 5 minutes. Next, samples were centrifuged using a mini-centrifuge at maximum speed. Then, samples were incubated with acetonitrile as described above. The solutions were then removed by pipetting after a quick spin using micro-centrifuge. Subsequently, gel plugs were dried and digested with 15  $\mu$ l trypsin (12.5 ng/ $\mu$ L Trypsin, 41.7 mM ABC, 4.17 mM  $\text{CaCl}_2$ ) overnight. The next day, the solution was collected by a quick spin using micro-centrifuge and a fine pipette tip. The solution was transferred to a clean 1.5 mL microcentrifuge. Subsequently, gel fragments were washed with acetonitrile as mentioned above. The sample was dried and incubated with 5% formic acid for 15 minutes at 37°C and 1,050 rpm in a thermoshaker. Then, the sample was incubated with 50  $\mu$ l acetonitrile at 37°C and 1,050 rpm in a thermoshaker. The gel plug was then spun down at maximum speed using a mini-centrifuge. The supernatant was collected and pooled with the supernatant from the digestion step. The combined supernatant was then evaporated using a speed vacuum (ThermoFisher Scientific, Savant™ SpeedVac™). Then, 30  $\mu$ l of the sample was loaded for mass spectrometry analysis on the ThermoScientific™ Orbitrap Fusion™ Tribrid™ mass spectrometer at the mass spectrometry facility, University of Lethbridge.

## **2.7 Western blot quantification**

The bands were quantified using an Amersham Imager 600 analysis software (GE healthcare). First, the number of lanes were chosen manually, and the bands were detected manually. The background was automatically subtracted by choosing the parameter 'rubber band'. The same method was followed for the loading control GAPDH. The ratio of the protein of interest and GAPDH was calculated. The quantitative analysis was performed for all three biological replicates. The graph was plotted for si-Control and si-hOLA1 using Graph Pad Prism7 software.

## Chapter 3: Results

### 3.1 hOLA1 depletion leads to upregulation of key anti-apoptotic proteins

As mentioned earlier, hOLA1 is known to suppress global protein synthesis by limiting ternary complex formation.<sup>136</sup> In addition, hOLA1 depletion is reported to result in a diminished ISR level and increased cellular survival.<sup>136</sup> ISR is known to play a key role in deciding cell fate through the effector proteins of ISR such as ATF4 and CHOP. These effector proteins are known to regulate several anti- and pro-apoptotic proteins.<sup>144, 145</sup> Therefore, I hypothesized that the reason for increased cellular survival in hOLA1-depleted cells is due to decreased apoptosis caused by the effect of diminished ISR level on the levels of anti-apoptotic proteins. Therefore, I wanted to assess the effect of hOLA1 removal in the cellular levels of key IAPs and anti-apoptotic proteins.

Breast cancer is one of the most aggressive and heterogeneous diseases.<sup>146</sup> hOLA1 is abnormally expressed in breast cancer.<sup>147</sup> One of the well-established breast cancer cell lines is MDA-MB231.<sup>146, 148, 149</sup> MDA-MB231 is a triple negative cell line, lacking progesterone receptor (PR) expression, human epidermal growth factor receptor 2 (HER2) and estrogen receptor (ER).<sup>149</sup> Moreover, Chen, H *et al.* have used MDA-MB231 cell line to investigate hOLA1 as a suppressor of protein synthesis and ISR regulator.<sup>136</sup> Hence, I wanted to study the role of hOLA1 in apoptosis using the MDA-MB231 cell line. First, I optimized the si-hOLA1 concentration and duration time for the effective knockdown with a minimum off-target effects on gene expression. To this end,  $1.5 \times 10^5$  MDA-MB231 cells were seeded in 6-well plates and transfected with two different concentrations of control siRNA and siRNA targeted against hOLA1 (25 nM, and 50 nM). 96 hours post-transfection, cells were lysed, and the cellular levels of proteins were analyzed by the

Western blot technique. The membrane was probed for hOLA1 and loading control glyceraldehyde 3-phosphate dehydrogenase (GAPDH). It is known that  $\alpha$ -actin interacts with hOLA1, therefore GAPDH was used as a loading control.<sup>150</sup> Following the incubation of the membrane with primary and secondary antibodies, the protein bands were visualized using an Amersham Imager 600 (GE healthcare). Subsequently, protein bands were quantified using the Amersham Imager 600 analysis software. Following the quantification, the relative expression was calculated by dividing the expression of hOLA1 by the expression of GAPDH in control siRNA and si-hOLA1 treated cells. The level of hOLA1 in control siRNA treated cells were considered as standard (100%) expression and the percent relative expression of hOLA1 was calculated. The numbers were plotted as bar graph using Prism Graph Pad software. According to the densitometry, cells treated with 25 nM of si-hOLA1 demonstrated 68% decrease in the level of hOLA1 compared to the control siRNA treated cells. However, when the cells were treated with 50 nM si-hOLA1, the protein expression level of hOLA1 was further decreased (almost 90%) (Figure 3.1). Therefore, I decided to use 50 nM si-hOLA1 for the rest of the study.



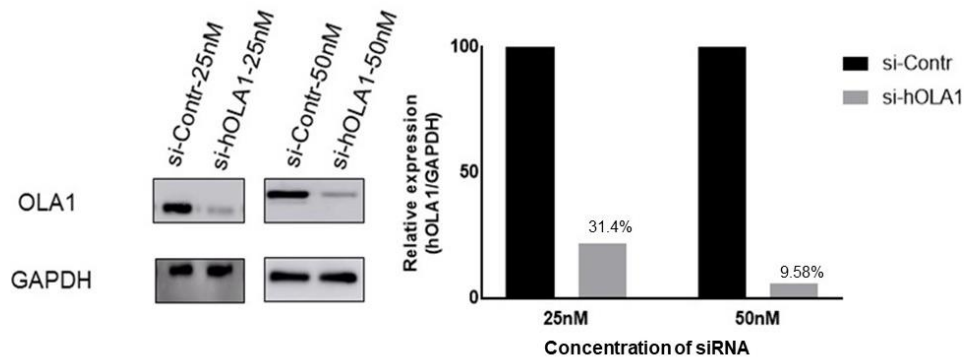


**Figure 3.1: Optimization of the concentration of si-hOLA1 for the depletion of hOLA1.** The expression of hOLA1 was depleted using 25 nM and 50 nM siRNA in MDA-MB231 cells. GAPDH was used as loading control. The relative expression of hOLA1 in control and si-hOLA1 transfected cells were quantified using Amersham 600 imager. According to the quantification, 25 nM si-hOLA1 demonstrated 68% decreased expression of hOLA1 compared to control siRNA treated cells. However, when 50nM si-hOLA1 was used, cells showed effective depletion (90%) of hOLA1 compared to 25 nM si-hOLA1 treated cells. siContr: control siRNA-treated cells, si-hOLA1: siRNA targeting hOLA1-treated cells.

Subsequently, I optimized the transfection duration time with the same cell line and cell number as described above; here I used 50 nM siRNA and different transfection time points (24h, 48h, 72h, and 96h). Cells were lysed, and the proteins were analyzed by the Western blotting technique. The relative band intensity of hOLA1 and GAPDH was quantified and analyzed as described above. According to the densitometry, 24 hours si-hOLA1 treated cells demonstrated 40% decrease in the expression of hOLA1 compared to control siRNA treated cells. However, when the transfection duration time was increased to 48,72 and 96 hours the protein level of hOLA1 was decreased by 60%, 80%, and 90% respectively (Figure 3.2). The better transfection duration for the effective knockdown was 96 hours (Figure 3.2). Therefore, I decided to use 50 nM siRNA and 96 hours transfection duration time for this study.

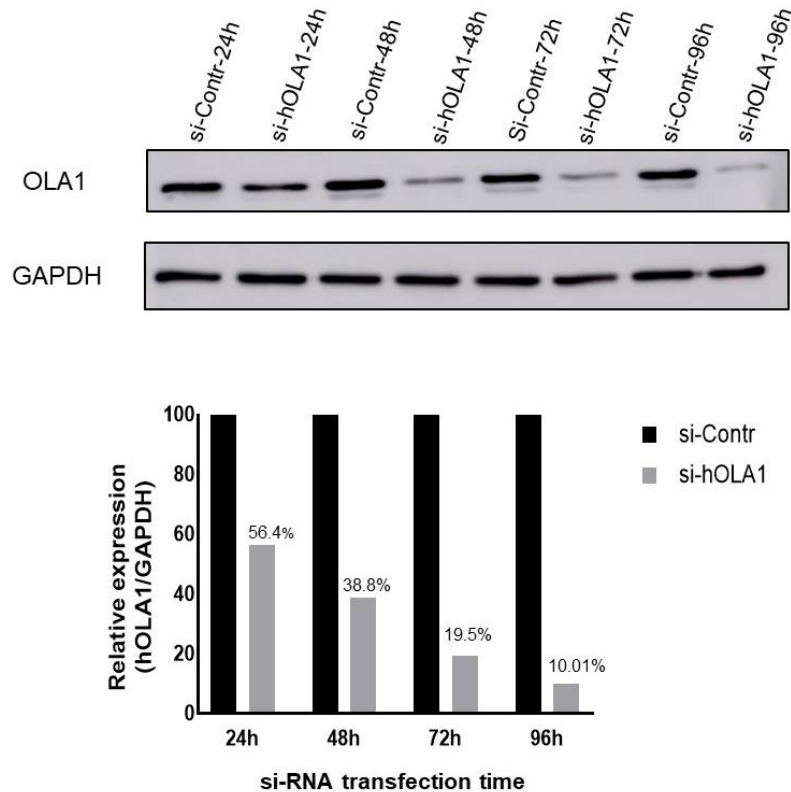


**Figure 3.2: Optimization of si-hOLA1 transfection duration time for the effective depletion.** hOLA1 was depleted using 50nM si-hOLA1 in MDA-MB231 cell line. GAPDH was used as loading control. The bands were quantified using Amersham 600 imager. According to the quantification, depending on the transfection duration time, hOLA1 expression was decreased by 40%, 60%, and 90% for 24, 48, and 96 hours transfection duration time respectively. The better hOLA1 depletion was observed at 96 hours post-transfection. siContr: control siRNA-treated cells, si-hOLA1: siRNA targeting hOLA1-treated cells.

As mentioned earlier, hOLA1 depletion leads to diminished ISR level and enhanced cell survival.<sup>136</sup> ISR is known to regulate apoptosis.<sup>50</sup> According to my hypothesis, increased cellular survival during hOLA1 depletion is due to decreased apoptosis caused by diminished ISR level. As mentioned in the introduction, CHOP is an effector protein of ISR and induced during ISR activation. Therefore, to verify that hOLA1 depletion leads to diminished ISR level and thus diminished CHOP level, I performed knockdown studies and Western blot analysis to assess the level of CHOP upon hOLA1 depletion. GAPDH

was used as the loading control. The level of CHOP is decreased in hOLA1-depleted cells compared to control cells (Figure 3.3). This suggests that hOLA1 depletion leads to decreased ISR level resulting in decreased level of CHOP in hOLA1-depleted cells (Figure 3.3).

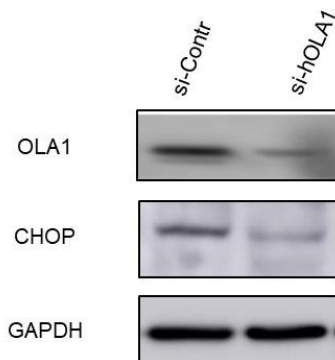


**Figure 3.3: hOLA1 depletion leads to diminished ISR.** The experiment was performed in MDA-MB231 cells using 50 nM siRNA and 96 hours post-transfection time. The cropped blot on the top represents successful hOLA1 depletion, middle blot implies the level of CHOP is decreased upon hOLA1 depletion. The third blot represents GAPDH, loading control to assess if equal lysates are loaded in all lanes. Decreased levels of CHOP in hOLA1-depleted cells suggests the diminished ISR levels upon hOLA1 depletion. siContr: control siRNA-treated cells, si-hOLA1: siRNA targeting hOLA1-treated cells.

As mentioned earlier, ISR regulates apoptosis through the regulation of anti- and pro-apoptotic proteins.<sup>50</sup> Therefore, I wanted to assess the effect of diminished ISR caused by hOLA1 depletion on the levels of key IAPs and anti-apoptotic proteins. To this end, hOLA1 was depleted using siRNA targeting hOLA1, and the levels of IAPs were assessed by Western blot analysis. The experiment was performed in two different cell lines: HEK-293T and MDA-MB231. I have used two different cell lines to verify if the role of hOLA1 in apoptosis is cell line specific or not. To this end, MDA-MB231 cells ( $1.5 \times 10^5$ ) and HEK-293T cells ( $1.0 \times 10^5$ ) were seeded and transfected with control siRNA and si-hOLA1. Cells were lysed 96 hours post-transfection and analyzed by Western blotting. The

membrane was probed for key anti-apoptotic proteins cIAP1, cIAP2, XIAP, cFLIP, and Bcl-xL.

The partial silencing of hOLA1 was verified by Western blotting (Figure 3.4). It is known that ISR regulates cIAP1.<sup>85</sup> Hence, first I assessed the level of cIAP1 upon hOLA1 depletion. cIAP1 is an inhibitor of the extrinsic apoptotic pathway. It inhibits apoptosis by interacting with extrinsic pathway signal transduction proteins TRAF1 and TRAF2 thus inhibiting the activation of caspase-8.<sup>108</sup> In addition, cIAP1 inhibits apoptosis by activation of RIP1 ubiquitylation.<sup>108</sup> Activation of RIP1 leads to RIPoptosome or complex II formation results in the activation of NF- $\kappa$ B pro-survival pathway.<sup>108</sup> The experiment was performed in three biological replicates. The bands were quantified using Amersham 600 software. The relative band intensity was calculated by dividing the protein of interest's expression by the expression level of the loading control (GAPDH). According to the densitometry, hOLA1-depleted cells demonstrated an increased level of cIAP1 compared to control cells in both cell lines. Error bars on the bar graph represent the standard error of the means. The reason for the variation between the biological replicates may be due to the saturated protein bands. This may show the higher variability among biological replicates and thus showing huge error bars. This suggests that there is a clear trend in the increase of cIAP1 levels by hOLA1 depletion. However, the statistical variability can be improved by avoiding saturation of protein bands. However, the level of cIAP1 in hOLA1-depleted cells is upregulated in all three biological replicates suggesting that hOLA1 depletion likely lead to upregulation of cIAP1 in MDA-MB231 and HEK-293T cell lines (Figure 3.4).

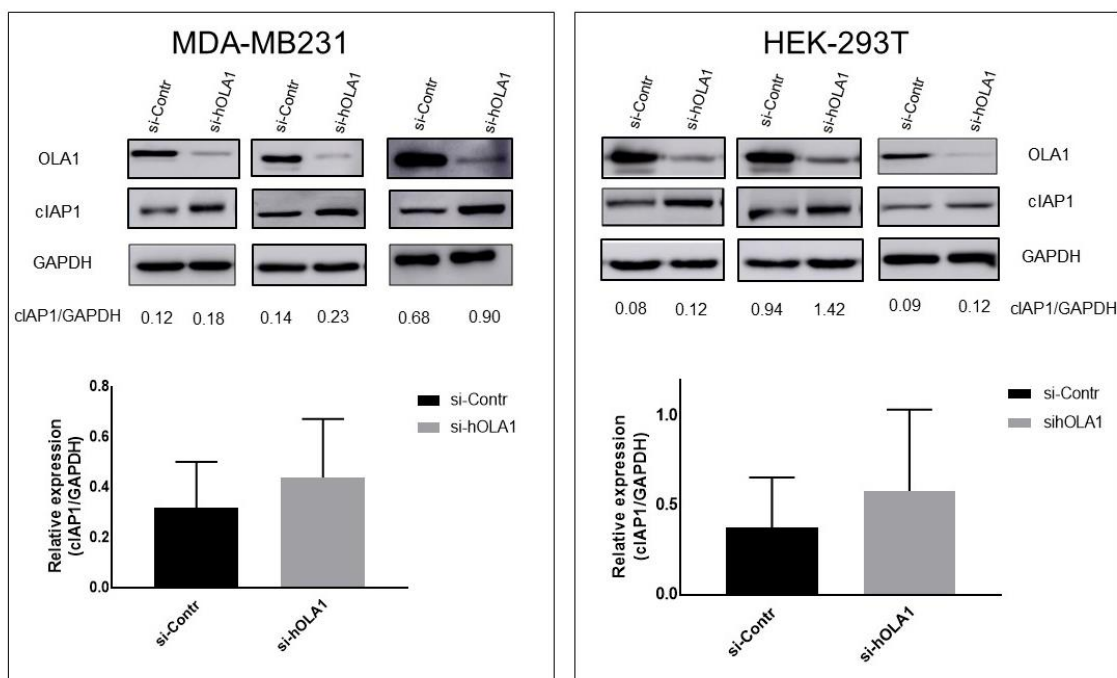


**Figure 3.4: hOLA1 depletion leads to increased levels of cIAP1 in MDA-MB231 and HEK-293T cell lines.** The left panel shows Western blot results from the MDA-MB231 cell line, and the right panel shows Western blot results from the HEK-293T cell line. hOLA1 was depleted in both cell lines and the membrane was probed for cIAP1 and GAPDH. The protein bands were quantified using Amersham 600 imager, and the numbers represent the ratio of cIAP1 to GAPDH. The relative expression was assessed, according to the quantification, hOLA1 depletion leads to increased levels of cIAP1 in both MDA-MB231 and HEK-293T cells. These Western blots are from three biological replicates. Error bars show the standard errors of the means (SEM). siContr: control siRNA-treated cells, si-hOLA1: siRNA targeting hOLA1-treated cells.

cIAP2 is a key anti-apoptotic protein and a homolog of cIAP1.<sup>108</sup> cIAP2 is known to be have functional redundancy with cIAP1.<sup>151</sup> Hence, I wanted to examine the levels of cIAP2 in hOLA1-depleted cells. hOLA1 was depleted in MDA-MB231 and HEK-293T cell lines. Subsequently, cell lysate was analyzed by Western blotting. The membrane was probed for cIAP2 and GAPDH. As described in the methods section, protein bands were quantified using an Amersham 600 Imager and the ratio of cIAP2 and GAPDH was assessed. The relative expression of cIAP2 was plotted using Prism Graph Pad. Error bars on the bar graph represent the standard error of the means. As mentioned earlier, some of the proteins

bands being saturated which may have resulted in a higher variability between biological replicates and thus showing huge error bars. However, according to the quantification, all three biological replicates of MDA-MB231 and HEK-293T cells suggest increased levels of cIAP2 upon hOLA1 depletion (Figure 3.5). The data indicate that hOLA1 depletion seems to upregulate cIAP2. However, this is not statistically significant. Taken together, hOLA1 depletion likely lead to the upregulation of cIAP1 and cIAP2.

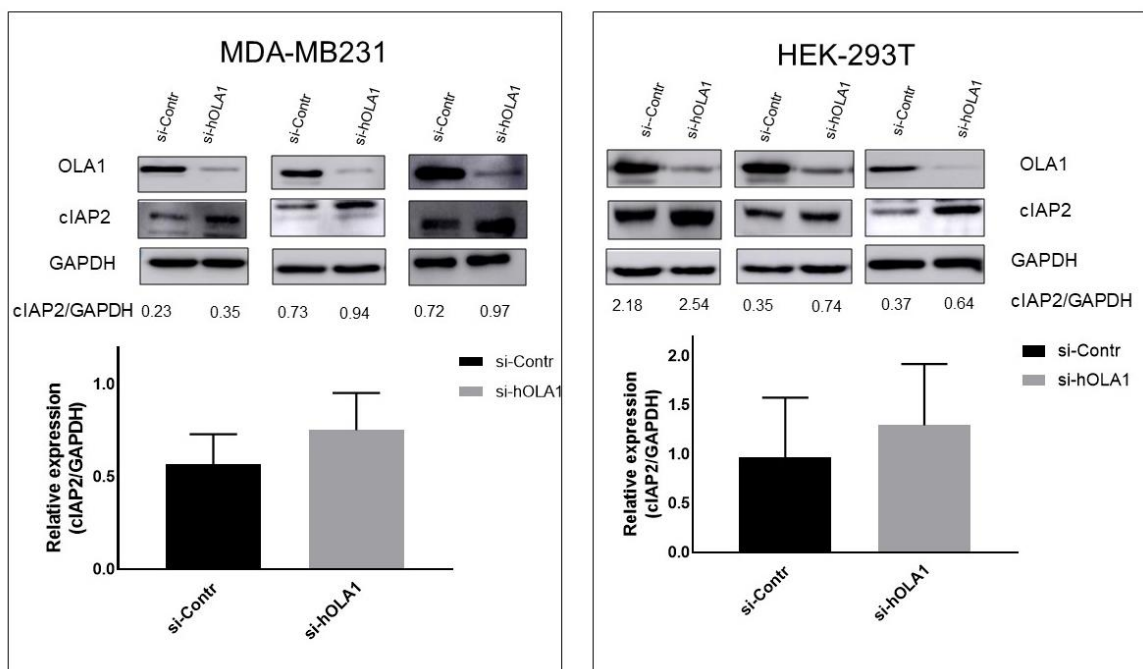


**Figure 3.5: hOLA1 depletion leads to increased levels of cIAP2 in MDA-MB231 and HEK-293T cell lines.** The left panel shows Western blot results from the MDA-MB231 cell line, and the right panel shows Western blot results from the HEK-293T cell line.

hOLA1 was depleted in both cell lines and the membrane was probed for cIAP2 and GAPDH. The protein bands were quantified using Amersham 600, the numbers represent the ratio of cIAP2 to GAPDH. According to the quantification, hOLA1 depletion leads to increased levels of cIAP2 in MDA-MB231 and HEK-293T cell lines. These Western blots are from three biological replicates. Error bars show SEM. siContr: control siRNA-treated cells, si-hOLA1: siRNA targeting hOLA1-treated cells.

Following that, I evaluated the levels of an anti-apoptotic protein that inhibits the extrinsic apoptotic pathway, cFLIP<sub>L</sub>. cFLIP inhibits apoptosis by competing with procaspase-8 to be

recruited onto the DISC.<sup>152</sup> Removal of hOLA1 did not show any considerable effect on the level of cFLIP splice variant cFLIP<sub>L</sub> in MDA-MB231 and HEK-293T cell lines (Figure 3.6). The middle blot of cFLIP<sub>L</sub> in HEK-293T was previously probed for cIAP2. The blot was not stripped and, like a cIAP2 antibody, the hOLA1 antibody was raised in rabbit, therefore it shows two bands (Figure 3.6, the middle blot in the right panel). The upper band was excluded during quantification. Error bars on the bar graph represent the standard error of the means. HEK-293T bar graph shows a huge error bar for the level of cFLIP<sub>L</sub> in hOLA1-depleted cells. This result may be due to the saturated cFLIP<sub>L</sub> band in the hOLA1-depleted cells (Figure 3.6, middle blot in the right panel). According to the quantification, hOLA1 depletion did not show any considerable effects on the level of cFLIP<sub>L</sub>.

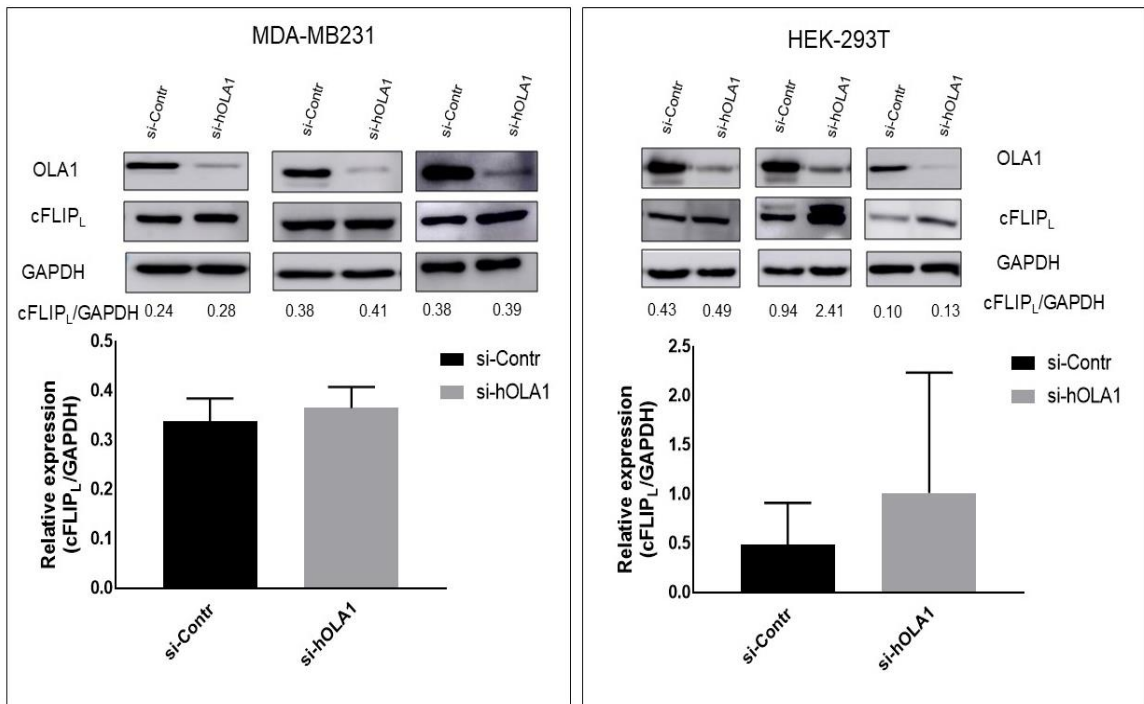


**Figure 3.6: hOLA1 depletion does not have a considerable effect on the levels of cFLIP<sub>L</sub> in MDA-MB231 and HEK-293T cell lines.** The left panel shows Western blot results from the MDA-MB231 cell line, and the right panel shows Western blot results from the HEK-293T cell line. hOLA1 was depleted in both cell lines and the membrane was probed for cFLIP<sub>L</sub> and GAPDH. The protein bands were quantified using Amersham 600 software, and the numbers represent the relative expression of cFLIP<sub>L</sub> and GAPDH. According to the quantification, hOLA1 depletion does not have a considerable effect on the level of cFLIP<sub>L</sub> in both cell lines. These Western blots are from three biological replicates. Error bars show SEM. siContr: control siRNA-treated cells, si-hOLA1: siRNA targeting hOLA1-treated cells.

It is known that removal of hOLA1 leads to diminished CHOP.<sup>136</sup> CHOP triggers apoptosis by repressing Bcl-2 family anti-apoptotic proteins.<sup>153</sup> Therefore, I evaluated the levels of the Bcl-2 family anti-apoptotic protein: Bcl-xL. Bcl-xL is crucial anti-apoptotic protein, that prevents pore formation on the mitochondrial membrane thus inhibit intrinsic and extrinsic apoptotic pathways.<sup>96</sup> The level of Bcl-xL was assessed by Western blotting. HEK-293T always produced double bands for Bcl-xL. When the control siRNA treated cells are compared to si-hOLA1 treated cells, the level of Bcl-xL seems to be upregulated



upon hOLA1 depletion in both cell lines (Figure 3.7). As mentioned earlier, some of the bands are saturated which may have resulted in a higher variability between biological replicates likely showing huge error bars.

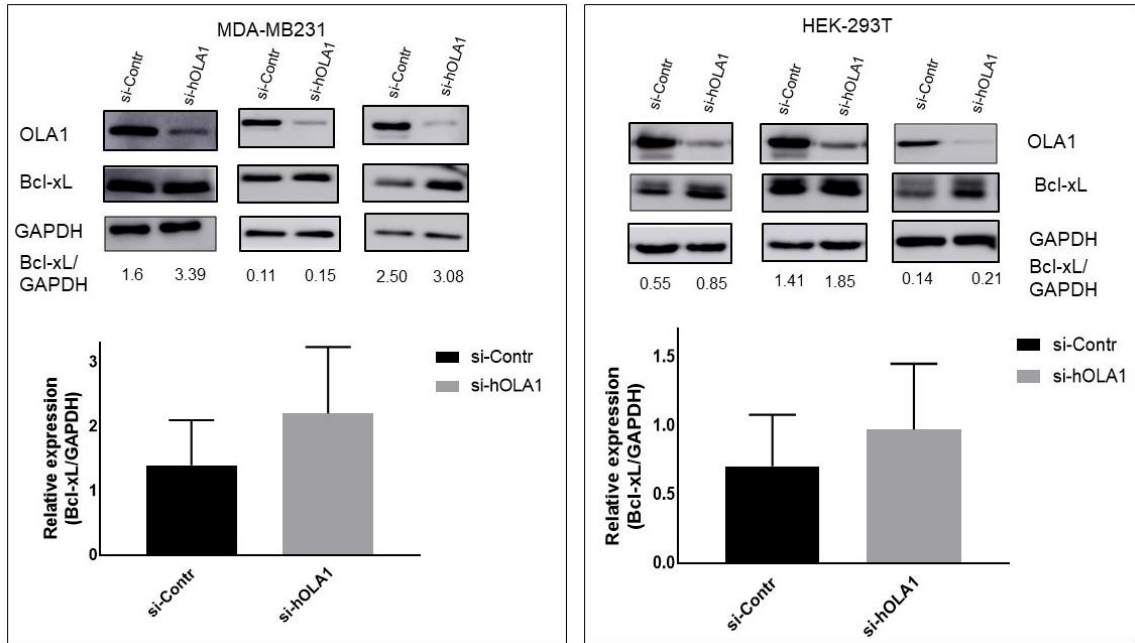


**Figure 3.7: hOLA1 depletion leads to increased levels of Bcl-xL in MDA-MB231 and HEK-293T cell lines.** The left panel shows Western blot results from the MDA-MB231 cell line, and the right panel shows Western blot results from the HEK-293T cell line. hOLA1 was depleted in both cell lines and the membrane was probed for Bcl-xL and GAPDH. The protein bands were quantified using Amersham 600 software, and the numbers represent the relative expression of Bcl-xL and GAPDH. hOLA1 depletion leads to upregulation of Bcl-xL in HEK-293T and MDA-MB231 cell lines. These Western blots are from three biological replicates. Error bars show the SEM. siContr: control siRNA-treated cells, si-hOLA1: siRNA targeting hOLA1-treated cells.

Previously it was reported that ATF4 regulates XIAP during ISR.<sup>78</sup> XIAP is known to inhibit both intrinsic and extrinsic apoptotic pathways by inhibiting caspase-9, caspase-3, and caspase-7.<sup>115</sup> Therefore, I wanted to assess the level of XIAP upon hOLA1 depletion. To this end, I performed hOLA1 depletion and Western blot analysis, and the relative expression was assessed as mentioned in the previous section. According to the quantification, there are no detectable changes in the levels of XIAP between control cells

and hOLA1-depleted cells in both cell lines (Figure 3.8). The reason for the variation between the biological replicates may be due to some of the protein bands being saturated which may have resulted in more variation between biological replicates likely showing huge error bars. Taken together, the findings of this section suggest that hOLA1 depletion likely leads to upregulation of key anti-apoptotic proteins: cIAP1, cIAP2, and Bcl-xL, but not XIAP or cFLIP<sub>L</sub>.

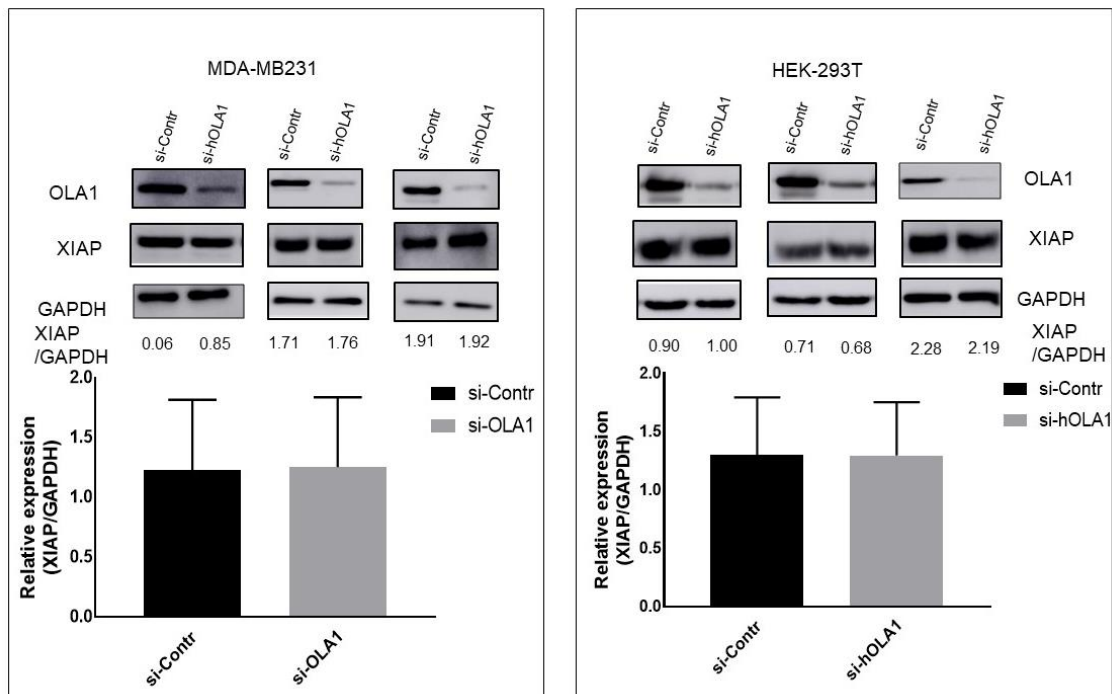


**Figure 3.8: hOLA1 depletion does not have a considerable effect on the levels of XIAP.** The left panel shows Western blot results from the MDA-MB231 cell line, and the right panel shows Western blot results from the HEK-293T cell line. hOLA1 was depleted in both cell lines and the membrane was probed for XIAP and GAPDH. The protein bands were quantified using Amersham 600 software, the numbers represent the relative expression of XIAP and GAPDH. According to the quantification, hOLA1 depletion doesn't have considerable changes on the level of XIAP in MDA-MB231 and HEK-293T cells. Error bars show SEM. siContr: control siRNA-treated cells, si-hOLA1: siRNA targeting against hOLA1-treated cells.

### **3.2 hOLA1 depletion leads to decreased caspase activation in the MDA-MB231 cell line.**

The previous section of this chapter shows that hOLA1 depletion might lead to upregulation of key anti-apoptotic proteins: cIAP1, cIAP2, and Bcl-xL. The major role of an anti-apoptotic protein is to inhibit caspase activation through direct and or indirect interactions. Therefore, I wanted to examine the cellular levels of initiator and executioner caspases in the combination of si-hOLA1 and apoptotic inducers treatment. In order to induce caspase activation, MDA-MB231 cells were treated with various apoptotic agents such as doxorubicin, TRAIL, and TNF $\alpha$ . Doxorubicin induces apoptosis by damaging DNA through intercalation and torsional stress while TRAIL and TNF- $\alpha$  induce apoptosis by binding to the receptors on the cell membrane.<sup>154, 155</sup> MDA-MB231 ( $1.5 \times 10^5$ ) cells were seeded in a 6-well plate, and hOLA1 was depleted using siRNA targeted against hOLA1. After 92 hours of siRNA treatment, cells were treated with 10 nM of doxorubicin, 100 ng/mL of TRAIL and 100 ng/mL of TNF $\alpha$  for 4 hours. Consequently, cells were lysed, and the proteins were analyzed by Western blotting. The membrane was probed for caspase-8, caspase-9, caspase-7, and caspase-3. In addition, the membrane was probed for cleaved PARP. PARP is a polymerase involved in DNA repair.<sup>156</sup> This protein is cleaved by caspase enzymes, therefore I wanted to assess the protein level of cleaved PARP by Western blotting.

The previous section suggests that hOLA1 depletion leads to upregulation of cIAP1, cIAP2, and Bcl-xL. As mentioned in the introduction, extrinsic anti-apoptotic proteins: cIAP1, and cIAP2 inhibit initiator caspase of the extrinsic pathway: caspase-8. Moreover, intrinsic apoptotic pathway activation could result in the activation of the extrinsic pathway. Intrinsic anti-apoptotic protein upregulation could also result in the inhibition of extrinsic

initiator caspase: caspase-8. Therefore, I assessed the level of caspase-8 upon hOLA1 depletion and apoptotic inducers treatment. When the membrane was probed for caspase-8, the cleaved caspase-8 level is higher in the combination of TRAIL and control siRNA compared to TRAIL combined with si-hOLA1. TRAIL is an extrinsic apoptotic pathway inducer, decreased caspase-8 cleavage may possibly due to the upregulation of extrinsic anti-apoptotic proteins such as cIAP1 and cIAP2 in hOLA1-depleted cells (Figure 3.9). However, executioner caspases: caspase-7 or caspase-3 did not show any detectable levels of activation. Nevertheless, the level of full-length caspase-7 seems to be increased in the cells treated with apoptotic agents and siRNA targeted against hOLA1 (Figure 3.9). This may possibly due to transcriptional or translation upregulation of caspase-7 upon hOLA1 depletion.<sup>157</sup> This may also possibly due to stabilization of caspase-7.<sup>158</sup> However, TNF $\alpha$  treated cells did not show detectable differences in the levels of cleaved caspase-8 (Figure 3.9). This may possibly due to the duration of TNF $\alpha$  treatment may not enough to induce caspase activation.

The intrinsic apoptotic pathway is mainly initiated through intrinsic pro-apoptotic proteins that leads to the activation of intrinsic initiator caspases and executioner caspases.<sup>89</sup> Previous section of this study suggests that hOLA1 depletion leads to increased levels of Bcl-xL. As mentioned earlier, Bcl-xL indirectly inhibits caspase-9 activation.<sup>108</sup> Therefore, I wanted to assess the protein level of caspase-9 upon hOLA1 depletion and apoptotic inducers treatment as described above. When the membrane was probed for caspase-9, an initiator caspase of the intrinsic apoptotic pathway, very faint cleaved caspase-9 was detected in the control lane treated with doxorubicin, whereas no detectable band was observed in si-hOLA1 combined with doxorubicin (Figure 3.9). This may possibly due to

the effect of increased Bcl-xL levels upon hOLA1 depletion. Increased levels of Bcl-xL may possibly have inhibited the activation of caspase-9 upon hOLA1 depletion. Interestingly, increased level of cleaved caspase-9 was observed in control cells treated with TRAIL compared to the combination of si-hOLA1 with TRAIL. As mentioned earlier in the introduction, TRAIL induces the activation of caspase-8. Activation of caspase-8 may result in the cleavage of Bid into t-Bid thus activating the intrinsic apoptotic pathway.<sup>105, 159</sup> Therefore, the increased level of cleaved caspase-9 is perhaps due to the crosstalk between intrinsic and extrinsic apoptotic pathways (Figure 3.9).

hOLA1 depletion resulted in the upregulation of anti-apoptotic proteins and the activation of caspase-8 and caspase-9. Activation of caspases leads to the cleavage of PARP.<sup>156</sup> PARP helps in the DNA repairing process during stress.<sup>156</sup> Therefore, I wanted to assess the level of cleaved PARP in the combination of si-hOLA1 and apoptotic inducers. When the membrane was probed for cleaved PARP, the level of PARP activation was inhibited in the combination of si-hOLA1-doxorubicin-treated cells compared to combination of siContra-doxorubicin-treated cells. Moreover, si-hOLA1-TRAIL-treated cells showed a clear inhibition of PARP activation compared to control si-RNA-TRAIL-treated cells. However, TNF $\alpha$  treatment does not show considerable PARP cleavage. This is perhaps due to the duration time of the TNF $\alpha$  treatment may not enough to induce apoptosis in the cells. Notably, TRAIL treatment shows more PARP cleavage compared to DNA damage inducer doxorubicin, this may possibly due to the effect of doxorubicin on PARP1 enzyme activity and expression.<sup>160</sup> Doxorubicin is known to induce the suppression of PARP1 enzyme activity and the expression, therefore we may see decreased level of cleaved PARP in doxorubicin treated cells.<sup>160</sup> Taken together, the data suggest that, hOLA1 depletion leads

to upregulation of anti-apoptotic proteins that may possibly result in the inhibition caspase activation.

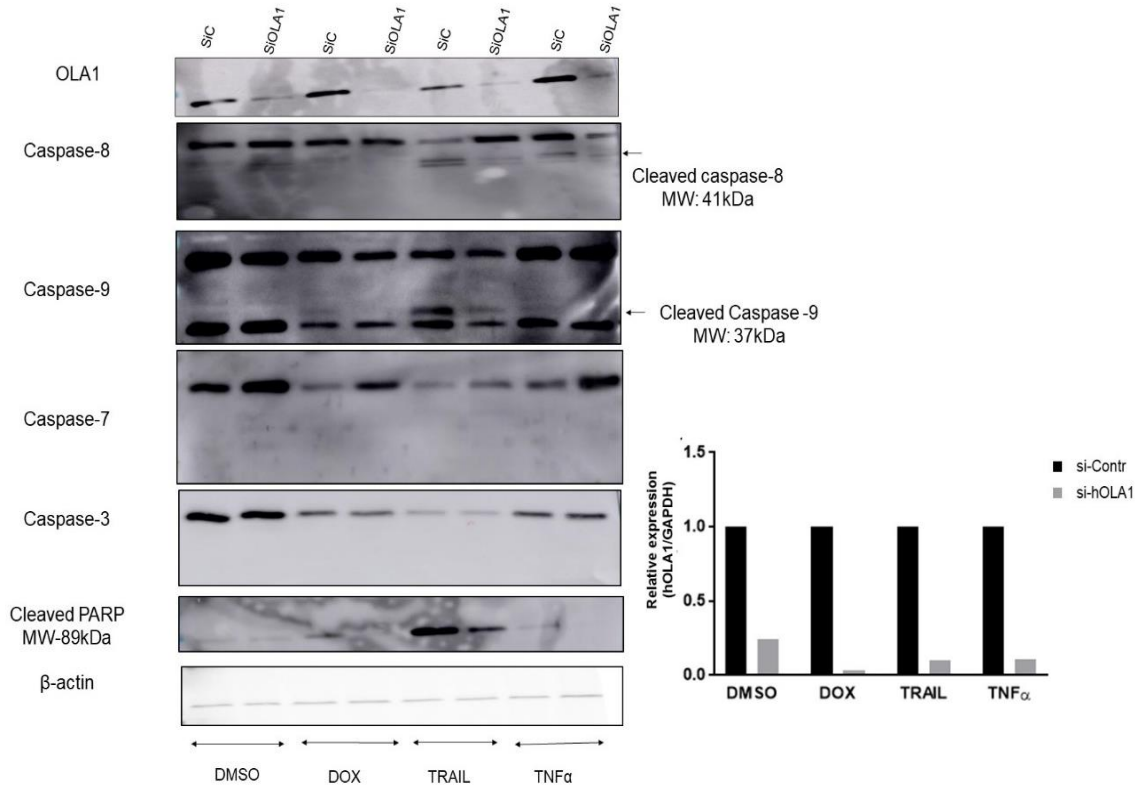


**Figure 3.9: hOLA1 depletion leads to decreased caspase activation.** hOLA1 was depleted in MDA-MB231 cells using siRNA transfection. DMSO was used as a control, and the cells were treated with 10 nM, 100 ng/mL, 100 ng/mL doxorubicin, TRAIL and TNF $\alpha$  respectively. Upon hOLA1 depletion and TRAIL treatment, cells showed decreased caspase-8 activity. Also, the level of cleaved PARP is decreased in hOLA1-depleted cells in the presence of apoptotic inducers, especially with TRAIL. The bar graph on the right represents the relative expressions of hOLA1 in all the treatment.

### 3.3. hOLA1 depletion does not have considerable effects on the inhibition of cell death

Previous experiments of this study showed that hOLA1 depletion leads to upregulation of key anti-apoptotic proteins such as cIAP1, cIAP2, and Bcl-xL. Also, hOLA1 depletion demonstrated a decreased caspase-8 activation upon apoptotic agent treatment. In addition, hOLA1 depletion and apoptotic agent treated cells demonstrated a decreased PARP

cleavage compared to control siRNA and apoptotic agent treated cells suggesting that hOLA1 depletion may inhibit apoptosis. Hence, I wanted to further examine the viability of hOLA1-depleted cells in the presence and absence of apoptotic inducers. The alamarBlue™ reagent was used to assess cell viability. MDA-MB231 cells ( $1 \times 10^4$ ) and HEK-293T cells ( $6 \times 10^3$ ) were seeded in a 96-well plate. Cells were treated with siRNA targeted against hOLA1 (si-hOLA1) and control siRNA (si-Cont). After 24 hours of siRNA treatment, cells were treated with apoptotic inducers (doxorubicin 10 nM, TRAIL 100 ng/mL, and TNF $\alpha$  100 ng/mL) for 72 hours. DMSO was used as a control because doxorubicin is dissolved in DMSO. Subsequently, the alamarBlue™ solution was added, and the fluorescence reading was measured using a fluorescent plate reader to measure cell viability.

In each biological replicate, all the treatments were normalized to control (DMSO). The average of three biological replicates was obtained. The differences between means were determined by the student t-test at  $P \leq 0.05$  using Graph Pad Prism software. According to the data from the MDA-MB231 cell line, there are no detectable differences in the viability between hOLA1-depleted cells and control cells in the absence of apoptotic agents (Figure 3.10). However, when the cells were treated with apoptotic agents such as TRAIL and TNF $\alpha$ , and si-hOLA1 shows a modest and statistically non-significant inhibition of cell death compared to control cells treated with the apoptotic agent. This modest difference may possibly be due to increased key anti-apoptotic proteins such as cIAP1 and cIAP2. When the cells were treated with intrinsic pathway apoptotic inducer doxorubicin, hOLA1-depleted cells exhibited a modest and statistically non-significant decrease in cell death.

This modestly decreased viability may possibly due to the upregulation of intrinsic anti-apoptotic protein Bcl-xL upon hOLA1 depletion.

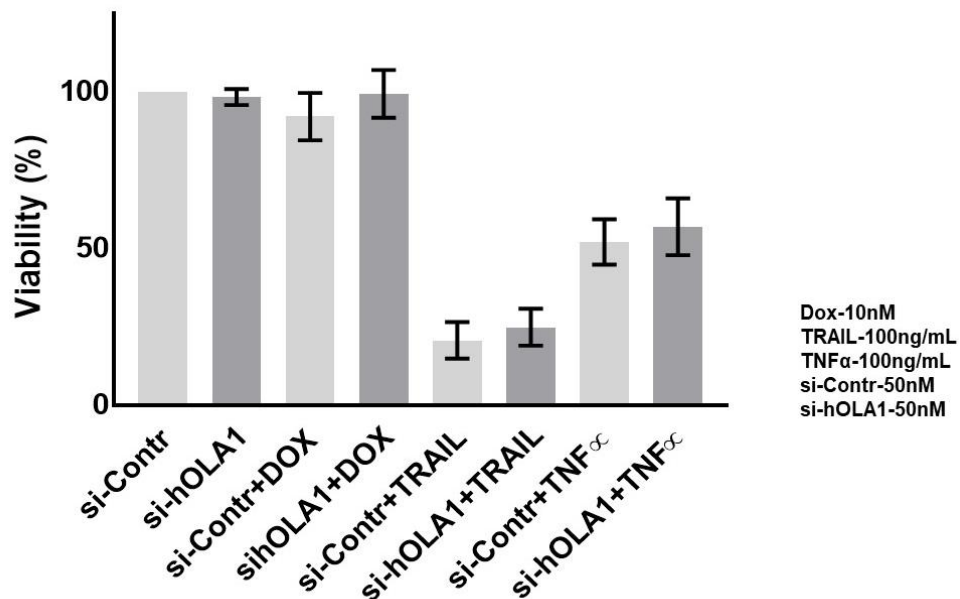


**Figure 3.10: hOLA1 depletion and apoptotic induction do not have considerable effects on the inhibition of cell death in MDA-MB231 cell line.** hOLA1 was depleted in MDA-MB231 cells using siRNA transfection. The light grey bar shows control siRNA treated cell viability and the dark grey bar shows hOLA1-depleted cell viability. DMSO was used as a control. The cells were treated with 10 nM doxorubicin, 100 ng/mL TRAIL, and 100 ng/mL TNF- $\alpha$ . The graph represents means of three biological replicates. Upon hOLA1 depletion and apoptotic inducers treatment, cells show modest inhibition of cell death. An unpaired t-test was used to detect significant differences at  $P \leq 0.05$ . The difference was found to be non-significant. Therefore, hOLA1 depletion and apoptotic induction do not have a considerable effect on the inhibition of cell death. The error bars represent the SEM.

The same experiment was performed in HEK-293T. HEK-293T cells showed similar trend like MDA-MB231. However, cells did not show a modest cell death inhibition upon hOLA1 depletion and apoptotic agent treatment like MDA-MB231. Notably, the alamarBlue™ assay may not represent the correct physiological state of the cell. For example, cells undergoing apoptosis may not be represented as dead in the alamarBlue™ assay. Therefore, the alamarBlue™ assay does not validate if the modest cell death



inhibition is due to decreased apoptosis. Hence, to validate that the increased cell survival upon hOLA1 depletion is due to the upregulation of anti-apoptotic proteins resulted in decreased apoptosis, I performed PI staining and flow cytometry.

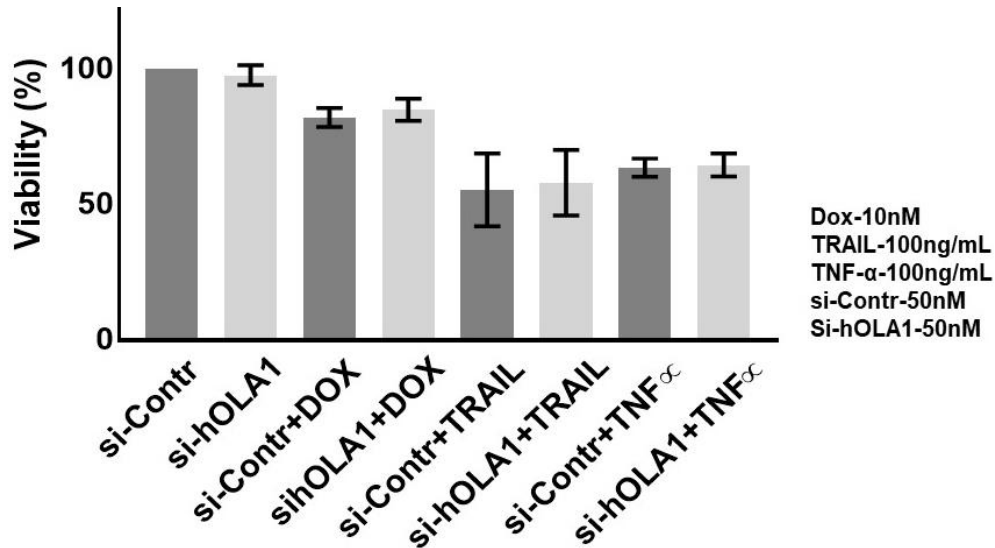


**Figure 3.11: hOLA1 depletion and apoptotic induction do not have considerable effects on cell death inhibition in HEK-293T cell line.** hOLA1 was depleted in HEK-293T cells using siRNA transfection. The light grey bar represents the viability of control siRNA treated cells, and the dark grey bar represents the viability of hOLA1-depleted cells. DMSO was used as a control, and the cells were treated with 10 nM doxorubicin, 100 ng/mL TRAIL, and 100 ng/mL TNF- $\alpha$ . The graph represents means of three biological replicates. Cells do not demonstrate any considerable effects on the inhibition of cell death upon hOLA1 depletion and apoptotic agent treatment. An unpaired t-test was used to detect significant differences at  $P \leq 0.05$ . Error bars represent the SEM.

### 3.4. Measurement of apoptosis in hOLA1-depleted cells

The PI staining experiment was performed using MDA-MB231 cells. MDA-MB231 ( $1.5 \times 10^5$ ) cells were seeded in a 6-well plate, and hOLA1 depletion was performed as described previously. At 92 hours of post-transfection, cells were treated with 100 ng/mL apoptotic inducer TRAIL. After 4 hours of treatment with TRAIL, cells were trypsinized and fixed in 70% ethanol overnight. Following that, cells were stained with PI staining and submitted for flow cytometry.

Apoptotic cells are characterized by DNA fragmentation and the loss of DNA content. PI is a fluorescent intercalating agent that can be used to label DNA and measure the cellular DNA content by flow cytometry analysis.<sup>161</sup> Hence, PI staining and flow cytometry analysis was used to measure apoptosis upon hOLA1 depletion. Apoptotic cells are represented in the sub G<sub>0</sub> phase because cells containing fragmented DNA would be in the G<sub>0</sub> phase. Due to some technical errors made in gating, I am presenting the data from two different biological replicates (control cells without apoptotic inducers and cells treated with apoptotic inducers). Hence, I did not compare control cells (no treatment) and apoptotic agent-treated cells. Based on the control cells treated with nocodazole, each phase was gated by the flow cytometry facility. From the histogram, the percentage of cells sub-population in each phase was obtained (Figure 3.12, numbers in each phase of the histogram). The control siRNA treated cells were considered as 100% and si-hOLA1 treated cells were normalized to control cells in each phase. The percentage of cells in each phase was plotted using Prism Graph Pad. The percentage of cells sub-population in each phase was compared between control siRNA and si-hOLA1 treated cells. From the bar graph on the left (representative of histogram) the proportion of cell number in G<sub>0</sub> phase was decreased in hOLA1-depleted cells. A 20% decrease in apoptosis (number of cells in the sub G<sub>0</sub>) was observed (Figure 3.12). Also, when cells treated with the combination of control siRNA and TRAIL were compared to cells treated with a combination of TRAIL and si-hOLA1, a 40% decrease in apoptosis was observed (Figure 3.12, the bar graph on the right). This data suggests that hOLA1 depletion leads to decreased apoptosis. Moreover, control siRNA treated cells (Figure 3.12, left-bar graph) demonstrated an increased proportion of the cells in G<sub>0</sub>/G<sub>1</sub> phase, suggesting that hOLA1 depletion leads to cell cycle arrest in G<sub>0</sub>/G<sub>1</sub> phase (Figure 3.12). This is possibly due to hOLA1's role as a suppressor

of p21.<sup>143</sup> Removal of hOLA1 leads to increased level of p21 thus causing a cell cycle arrest in the G<sub>0</sub>/G<sub>1</sub> phase.<sup>143</sup> However, a combination of si-hOLA1 and apoptotic agent treatment did not demonstrate a cell cycle arrest in G<sub>0</sub>/G<sub>1</sub> phase. This may be possibly due to the effect of TRAIL treatment. hOLA1 depletion demonstrated a decreased proportion of the cell number S and G<sub>2</sub>/M phase. The same trend was observed for S and G<sub>2</sub>/M phase in hOLA1-depleted-TRAIL-treated cells. Together the findings of my study suggest that hOLA1 depletion leads to upregulation of anti-apoptotic proteins such as cIAP1, cIAP2, and Bcl-xL thus possibly decreases caspase activation and apoptosis.

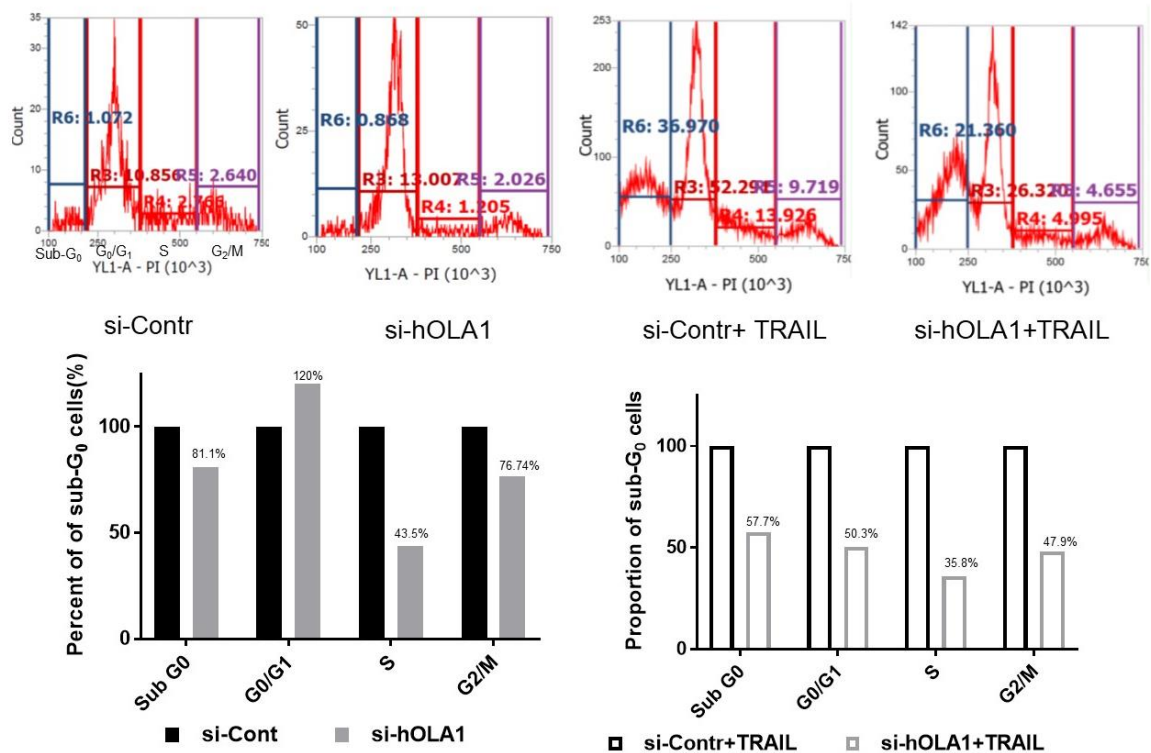


**Figure 3.12: hOLA1 depletion leads to decreased apoptosis.** hOLA1 was depleted in MDA-MB231 cell line using si-hOLA1. From the data file, DNA content from each phase in the histogram was plotted and represented as a bar graph. DNA content represents the proportion of the number of cells in each phase. According to the bar-graph hOLA1- depleted cells showed a 20% decrease in the number of apoptotic cells compared to control cells. The bar graph on the right side shows cells treated with 100 ng/mL TRAIL. Upon hOLA1 depletion and TRAIL treatment, cells showed 40% decrease in the number of apoptotic cells (sub-G<sub>0</sub> cells).

### **3.5 Co-immunoprecipitation and mass spectrometry to identify the protein(s) interacting with hOLA1**

As mentioned earlier, hOLA1 interacts with eIF2 and inhibits global translation.<sup>136</sup> However, it remains unclear as to how hOLA1 interacts with eIF2.<sup>136</sup> The interaction of hOLA1 with eIF2 could be regulated by additional protein(s). To identify the protein(s) interacting with hOLA1, I performed co-immunoprecipitation of hOLA1 using MDA-MB231 cells followed by mass spectrometry. Cells were lysed when they reached 80% confluency using the RIPA lysis buffer. Subsequently, the lysate was incubated with anti-hOLA1 antibody-coated beads for 3 hours at 4°C. A portion of IP eluate was subjected to SDS-PAGE separation and stained with Coomassie stain in preparation for the mass spectrometry analysis. Protein bands were then excised and submitted for mass spectrometry.

The pull-down of hOLA1 was validated by Western blotting using the remaining portion of IP eluate, then the membrane was probed for Anti-hOLA1 antibody (Figure 3.13, left panel). The same membrane was probed for eIF2 $\alpha$ . However, as mentioned by Chen, H *et al.*<sup>136</sup> I did not see the eIF2 $\alpha$  interaction of hOLA1 with endogenous IP using anti-hOLA1 antibody. On the Coomassie-stained gel, I observed two bands, one at about 45kDa (Sample I), and the other at about 150kDa (Sample II). I anticipated the protein observed at about 45kDa could be hOLA1 (MW:42kDa). Hence I excised both bands and submitted them for mass spectrometry. The mass spectrometry resulted in many hits for both samples. I looked at the molecular weight of excised band corresponding to the given hits and higher coverage (coverage is the percentage of the protein sequence covered by all identified peptides in the sample). Next, I checked sequence similarity between the proteins similar to hOLA1's

molecular weight with hOLA1's sequence using basic local alignment search tool (BLAST) in National Center for Biotechnology Information (NCBI). As a result, the protein similar to hOLA1's molecular weight had 90% coverage from mass spectrometry and 67% similarity with hOLA1. This strongly suggests that hOLA1 is pulled down. Next, I assessed the hits received for sample II, according to the molecular weight and the better coverage. Three hits demonstrate a similar molecular weight as sample II and better coverages such as Ubiquitin C, Rho-associated protein kinase, and Actin like filament (FLJ00119) (Table 3.2). The Ubiquitin C variant protein demonstrates higher coverage (40%) compared to the other two. It is known that hOLA1 protects HSP70 from ubiquitylation-mediated protein degradation.<sup>137</sup> Hence, it is possible that hOLA1 may interact with Ubiquitin C variant and prevent ubiquitylation-mediated degradation. However, the interaction of hOLA1 with Ubiquitin C variant needs to be further validated by reciprocal IP and Western blotting. The Rho-associated protein kinase and Actin like filament (FLJ00119) demonstrate similar molecular weight and 2% or 5% coverage respectively. Rho-associated protein kinase and Actin like filament (FLJ00119) are known to be involved in cell adhesion.<sup>162</sup> It is previously reported that hOLA1 negatively regulates cell adhesion.<sup>137</sup> Taken together, the data of IP and mass spectrometry suggests that hOLA1 may not strongly interact with the  $\alpha$  subunit of eIF2 as previously reported by Chen, H *et al.*<sup>136</sup> Also, hOLA1 may possibly interact with Ubiquitin C variant or Rho-associated protein kinase or Actin like filament and negatively regulate cell adhesion.

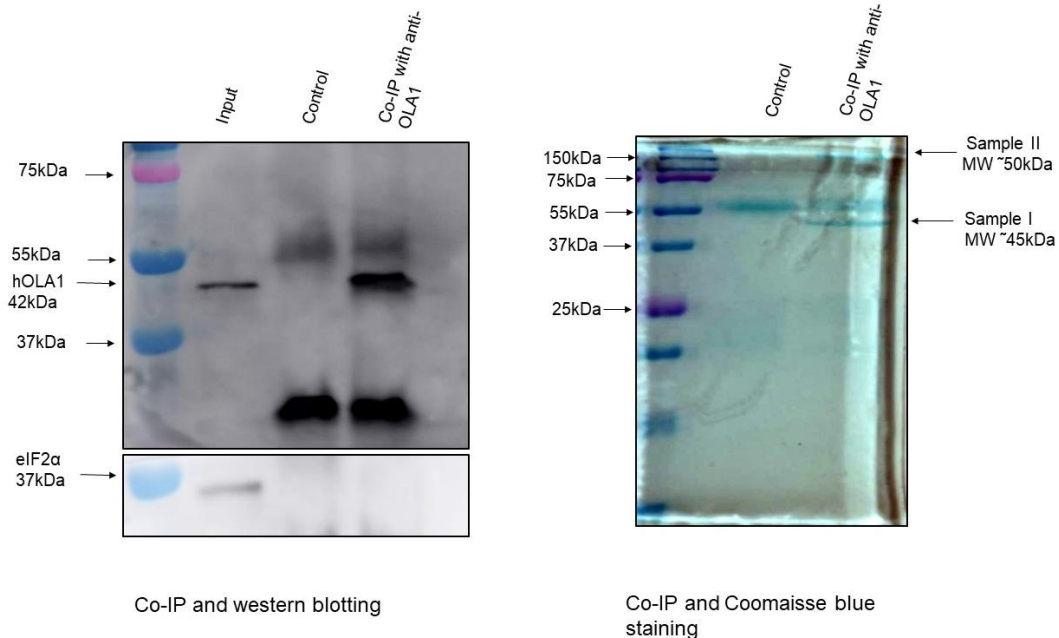


**Figure 3.13: Co-immunoprecipitation to identify the protein(s) interacting with hOLA1.** The left image shows the western blot analysis of hOLA1 immunoprecipitation. The first lane represents the whole cell lysate, second lane represents the control-IP and the third lane represents the hOLA1-IP. The protein band at 42kDa in third lane validates the pulldown of hOLA1. The right image represents the SDS-PAGE and Coomassie staining. The observed bands on the Coomassie-gel (sample I and II) were excised and analyzed by mass-spectrometry.

**Table 3.1: Mass spectrometry data analysis of sample I (MW ~45kDa).** Hits with higher coverage and similar molecular weight of hOLA1 were assessed for sequence similarities with hOLA1 to see if the pull-down is worked. There is a 64%-67% sequence similarity between hOLA1 and mass spectrometry hits with higher coverage and similar molecular weight validating the pulldown of hOLA1 has worked.

Hits (coverage)	MW(kDa)	Sequence similarity with hOLA1
Putative uncharacterized protein (91%)	40.4	67% Identity
Guanine nucleotide-binding protein G (87%)	40.7	64% Identity

**Table 3.2: Possible interacting partner of hOLA1.** Mass spectrometry data for sample II. Hits with higher coverage and similar MW of sample II from the mass spectrometry data is listed on the table. These proteins are previously reported to be involved in cell adhesion. hOLA1 negatively regulates cell adhesion. This suggests that hOLA1 was successfully pulled-down and it could interact with one of the proteins listed above.

<b>Hits(coverage)</b>	<b>MW(kDa)</b>	<b>Known roles of hOLA1 of the hits</b>
Ubiquitin C variant (40%)	147.25	hOLA1 is known to prevent HSP70 from ubiquitylation-mediated degradation
Rho-associated protein kinase (2%)	158	hOLA1 is a negative regulator of cell adhesion
Actin like filament (FLJ00119) (5%)	158	hOLA1 is a negative regulator of cell adhesion.

## **Chapter 4: Discussion and future directions**

### **4.1 Discussion**

hOLA1 is known to have numerous roles in tumor progression like cancer metastasis, and inhibition of centrosome regulation.<sup>135, 137, 138, 143</sup> Moreover, hOLA1 is reported to exhibit a regulatory effect on the global mRNA translation.<sup>136</sup> hOLA1 suppresses translation initiation by inhibiting ternary complex formation, and removal of hOLA1 leads to enhanced cellular survival and diminished ISR.<sup>136</sup> Decreased level of ISR leads to diminished ISR effector proteins: ATF4 and CHOP.<sup>163</sup> Depending on the type of the stress condition, ATF4 and CHOP regulate pro-apoptotic genes at the transcription level (Bcl-2) and anti-apoptotic proteins.<sup>85, 164</sup> Therefore, I hypothesized that increased cell survival upon hOLA1 depletion is due to decreased apoptosis caused by the effect of diminished ISR on anti-apoptotic proteins. In this study, I evaluated the role of hOLA1 in apoptosis by assessing the levels of anti-apoptotic proteins, caspase activation and measuring apoptosis.

Diminished ISR in hOLA1-depleted cells was verified by assessing the levels of CHOP (Figure 3.3). Removal of hOLA1 resulted in decreased CHOP levels (Fig. 3.3) and upregulation of key anti-apoptotic proteins; cIAP1, cIAP2, and Bcl-xL (Figures: 3.4, 3.5, 3.7 respectively). Previous studies have reported that ISR plays a crucial role in regulating cellular survival and cell death pathways depending on the type of stress condition.<sup>38</sup> CHOP and ATF4 is known to have numerous roles in promoting and inhibiting apoptosis by regulating anti- and pro-apoptotic proteins as described below.<sup>165</sup>

During chronic PERK signaling, ATF4-CHOP signaling is reported to show decreased levels of the IAPs: cIAP1, cIAP2, Livin, and Survivin.<sup>78</sup> Furthermore, PERK signaling leads to decreased synthesis of XIAP through dysregulation of cap-dependent translation.<sup>78</sup>



Also, increased levels of ATF4 during PERK mediated ISR promotes proteasomal degradation of XIAP through ubiquitylation resulting in decreased XIAP level.<sup>78</sup> Moreover, CHOP is a direct target of Bcl-2 family proteins.<sup>166</sup> CHOP-mediated apoptosis is known to be inhibited by anti-apoptotic protein: Bcl-xL and CHOP are known to promote the expression of pro-apoptotic proteins: DR5 and Bax.<sup>166, 167</sup> Moreover, CHOP is known to be degraded by cIAP1 and CHOP degrades cFLIP<sub>L</sub> through ubiquitylation and proteasome degradation.<sup>144, 145</sup> Together, all these previous studies of ATF4-CHOP mediated regulation of anti- and pro-apoptotic proteins suggesting that decreased CHOP levels could be the reason for the upregulation of anti-apoptotic proteins upon hOLA1 depletion. Hence, I propose that upregulation of anti-apoptotic proteins: cIAP1, cIAP2, and Bcl-xL may possibly occur due to the diminished levels of CHOP and ATF4 caused by hOLA1 depletion.

On the other hand, hOLA1 is known to regulate the expression of heat shock protein 70 (HSP70).<sup>137</sup> HSP70 is stress response protein that has the cellular defense mechanism against environmental stresses.<sup>137</sup> HSP70 is known to inhibit apoptosis by interacting with APAF1.<sup>168</sup> hOLA1 prevents ubiquitylation mediated degradation of HSP70 by replacing the E3 ubiquitin ligase: C-terminus of Hsc70-interacting protein (CHIP) at the carboxyl-terminus of HSP70.<sup>137</sup> Therefore, hOLA1 may have a direct or indirect interaction with anti-apoptotic proteins leading to the inhibition of its function. Hence, hOLA1 may negatively regulate anti-apoptotic proteins independent of CHOP and ATF4. It is also possible that the upregulation of cIAP1 and cIAP2 upon hOLA1 depletion leads to the activation of the NF- $\kappa$ B pro-survival pathway, resulting in the enhanced cellular survival.<sup>169</sup>

Notably, when I performed Western blot analysis in order to assess the levels of anti-apoptotic proteins upon hOLA1 depletion, some of the bands were too saturated. This may have been caused by issues related to Western blotting such as immunoprobings, membrane transfer, concentrated antibody or increased exposure time of the blot in the imaging system. Different type of optimization step may reduce the saturation of bands such as linearity test of the antibody with different concentration of the proteins and varying exposure time of the blots while imaging.<sup>170</sup>

The major function of an anti-apoptotic protein is to inhibit apoptosis by directly or indirectly inhibiting caspase activation.<sup>108</sup> Inhibitors of extrinsic apoptotic pathway cIAP1 and cIAP2 inhibit caspase-8 and caspase-10.<sup>108</sup> TRAIL induces extrinsic apoptotic pathway by binding to the receptor on the cell membrane.<sup>155</sup> In this study, activation of caspases was assessed by evaluating the cellular levels of cleaved caspases. Figure 3.9 demonstrates increased level of caspase-8 activation in control siRNA-TRAIL-treated cells compared to si-hOLA1-TRAIL-treated cells. This suggests that increased levels of extrinsic inhibitors of apoptosis proteins cIAP1 and cIAP2 may have resulted in decreased caspase-8 activation upon hOLA1 depletion and TRAIL treatment. Notably, cleaved caspase-9 was reduced in hOLA1-depleted-TRAIL-treated cells compared to control siRNA-TRAIL-treated cells, suggesting that this effect is possibly due to the crosstalk between the extrinsic and intrinsic apoptotic pathways. Caspase-8 may cleave Bid into truncated Bid (t-Bid) thus activating the intrinsic pathway of apoptosis.<sup>105</sup> However, this needs to be verified by assessing the cellular levels of Bid and tBid by Western blotting. Notably, PARP is a DNA repairing enzyme, however, when the cells were treated with DNA damaging agent doxorubicin, the western blot image did not demonstrate considerable PARP cleavage, this could possibly

due to doxorubicin is known to induce the suppression of PARP1 enzyme activity and the expression thus showing decreased PARP level (Figure 3.9).<sup>160</sup>

Furthermore, viability assay to assess the effects of hOLA1 depletion revealed that depletion of hOLA1 demonstrates modest inhibition of cell death in the presence of apoptotic inducers. However, the western image did not show considerable inhibition of cell death. This could be due to variable reason: cells were treated with apoptotic agents for 72 hours. Even though hOLA1 depletion leads to the upregulation of anti-apoptotic proteins when cells were treated with apoptotic inducers like TRAIL they undergo lots of other stresses like oxidative stress and plasma membrane depolarization.<sup>171</sup> Therefore, the upregulation of anti-apoptotic proteins may not enough to overcome the effect of the apoptotic inducers treatment. Moreover, TNF $\alpha$  induces cell survival pathway through cFLIP<sub>L</sub> activation.<sup>152</sup> This is perhaps a reason for the failure of hOLA1-depleted cells to demonstrate considerable difference in the cell viability compared to control cells and caspase-8 activation (Figure 3.9, 3.10 and 3.11). Also, doxorubicin treated cells did not show considerable cell death compared to cells treated with DMSO (control cells) in viability assay. It may possibly due to the concentration of doxorubicin may not enough to induce cell death. As mentioned earlier, the alamarBlue™ assay may not represent cells undergoing apoptosis. Therefore, I performed PI staining and flow cytometry to show that hOLA1 depletion leads to inhibition of cell death. The results of PI staining and flow cytometry analysis demonstrate that hOLA1 depletion leads to inhibition of apoptosis.

The mechanism of how hOLA1 inhibiting TC and the interaction with eIF2 is still unclear.<sup>129</sup> In order to identify the protein(s) interacting with hOLA1, I attempted to perform IP and mass spectrometry. To verify the pull-down and interaction of hOLA1 with

eIF2 $\alpha$  as mentioned by Chen, H *et al.*, I performed Western blotting with a portion of the IP sample. When I probed the membrane with anti-hOLA1 and anti-eIF2 $\alpha$  antibody, I did not detect eIF2 $\alpha$  as mentioned by Chen, H *et al.*<sup>136</sup> Notably, Chen, H *et al.* did not validate the interaction of hOLA1 with eIF2 $\alpha$  by endogenous IP of hOLA1.<sup>136</sup> The reason for not detecting the interaction of hOLA1 with eIF2 $\alpha$  by Western blotting may possibly due to weak interaction of eIF2 $\alpha$  with hOLA1, or hOLA1 may not interacting with  $\alpha$  subunit of eIF2, it could possibly interact with GTP binding subunit of eIF2:  $\gamma$  subunit. In future, the interaction of eIF2 and hOLA1 can be assessed by crosslinking IP and Western blotting. Mass spectrometry analysis resulted in three possible proteins for the interacting partner of hOLA1: Ubiquitin C, Rho-associated protein kinase and Actin like filament (FLJ00119) (Table 3.1). hOLA1 is known to regulate cell adhesion and prevent HSP70 ubiquitylation-mediated protein degradation.<sup>150</sup> Rho-associated protein kinase and Actin like filament (FLJ00119) are known to involved in cell adhesion.<sup>162</sup> Ubiquitin C is involved in ubiquitylation-mediated protein degradation.<sup>172</sup> Therefore, it is possible that one of these proteins interacts with hOLA1 and regulate cell adhesion or protein degradation.<sup>162</sup> Taken together, this study suggests that hOLA1 depletion leads to upregulation of anti-apoptotic proteins such as cIAP1, cIAP2, Bcl-xL and decreased caspase activation resulting in decreased apoptosis.

## 4.2 Future perspective

hOLA1's roles as a protein synthesis suppressor and ISR regulator provide a different aspect of hOLA1's role in cell survival.<sup>136</sup> My study suggests that hOLA1 depletion inhibits apoptosis through upregulation of anti-apoptotic proteins such as; cIAP1, cIAP2, and Bcl-xL. However, further validation of the role of hOLA1 in anti-apoptotic protein regulation by overexpression of hOLA1. In order to effectively conclude that hOLA1 depletion inhibits apoptosis, it needs to be assessed as to if hOLA1 negatively regulate anti-apoptotic proteins independent of CHOP. Further, is this effect exerted due to the diminished CHOP level caused by hOLA1 depletion? Additional studies are required to validate the effect of hOLA1 removal on anti-apoptotic proteins in two conditions: CHOP overexpression and CHOP downregulation. Moreover, the effect of hOLA1 depletion in transcription and translation of anti-apoptotic proteins needs to be studied further. This can be studied by measuring the steady-state levels of mRNAs encoding anti-apoptotic proteins by qPCR. Polysome profiling study is required to validate if hOLA1 is translationally regulating anti-apoptotic proteins.

It would be interesting to assess the combination of hOLA1 depletion and Thapsigargin treatment (ISR inducer) and analyze at the levels of anti-apoptotic proteins. Following the treatment of the cells with this compound, assessing levels of CHOP and of anti-apoptotic proteins by Western blotting or qPCR will reveal if the effect is CHOP dependent or not. An important question arising from this study is how cIAP1 and cIAP2 are upregulated at the same time, it is known that cIAP1 and cIAP2 have functional redundancy.<sup>108</sup> The survival pathway NF- $\kappa$ B is regulated by the expression of both cIAP1 and 2. Therefore, I

suggest that hOLA1 may have some role in modulating NF- $\kappa$ B pro-survival pathway. This can be assessed by the mRNA and protein levels of survival pathway protein(s).

Furthermore, co-IP and mass spectrometry to assess the additional protein(s) interacting with hOLA1 was inconclusive as it was done only once. If we want to confirm and study further the interaction between the proteins pulled down with hOLA1, we can perform co-IP with overexpression of hOLA1. Overexpression of hOLA1 can be achieved by introducing a vector containing hOLA1 (For example FLAG-tag protein) by transfection. Following overexpression of hOLA1, IP, Western blotting and mass spectrometry may reveal the interaction of the unknown protein. Furthermore, pull-down can be verified by Western blotting with the antibody against the pulled down protein (mass spectrometry hits) and hOLA1. Moreover, the interaction between hOLA1 and eIF2 $\alpha$  can be validated by *in vitro* assays: for example, this interaction can be investigated by purifying each subunit of eIF2. These subunits can be incubated with hOLA1, and subsequent protein-pulldown will reveal the interacting partner of eIF2 with hOLA1.<sup>173</sup>

In future, this study can be further advanced using xenograft and syngeneic mouse models.<sup>174</sup> It is important to study the effect of overexpression of hOLA1 and tumor progression as we propose that hOLA1 promotes apoptosis. Hence overexpression of hOLA1 may result in decreased cancer progression. It would be interesting to see the synergistic effect of hOLA1 overexpression and anti-cancer drug treatment in tumorigenesis. Moreover, expression levels of hOLA1 in different types of cancer and the reason for aberrant expression need to be elucidated as since it can serve as a tumor marker. In conclusion, hOLA1 may represent a potential therapeutic target for cancer.

## References

1. Crick, F. Central dogma of molecular biology. *Nature* **227**, 561-563 (1970).
2. Robichaud, N. & Sonenberg, N. Translational control and the cancer cell response to stress. *Curr Opin Cell Biol* **45**, 102-109 (2017).
3. Dinman, J.D. Control of gene expression by translational recoding. *Adv Protein Chem Struct Biol* **86**, 129-149 (2012).
4. Day, D.A. & Tuite, M.F. Post-transcriptional gene regulatory mechanisms in eukaryotes: an overview. *J Endocrinol* **157**, 361-371 (1998).
5. Aitken, C.E. & Lorsch, J.R. A mechanistic overview of translation initiation in eukaryotes. *Nat Struct Mol Biol* **19**, 568-576 (2012).
6. Merrick, W.C. Cap-dependent and cap-independent translation in eukaryotic systems. *Gene* **332**, 1-11 (2004).
7. Pestova, T.V. & Kolupaeva, V.G. The roles of individual eukaryotic translation initiation factors in ribosomal scanning and initiation codon selection. *Genes Dev* **16**, 2906-2922 (2002).
8. Groppo, R. & Richter, J.D. Translational control from head to tail. *Curr Opin Cell Biol* **21**, 444-451 (2009).
9. Paulin, F.E., Campbell, L.E., O'Brien, K., Loughlin, J. & Proud, C.G. Eukaryotic translation initiation factor 5 (eIF5) acts as a classical GTPase-activator protein. *Curr Biol* **11**, 55-59 (2001).
10. Passmore, L.A. *et al.* The eukaryotic translation initiation factors eIF1 and eIF1A induce an open conformation of the 40S ribosome. *Mol Cell* **26**, 41-50 (2007).
11. Sokabe, M. & Fraser, C.S. Human eukaryotic initiation factor 2 (eIF2)-GTP-Met-tRNAi ternary complex and eIF3 stabilize the 43 S preinitiation complex. *J Biol Chem* **289**, 31827-31836 (2014).
12. Kahvejian, A., Svitkin, Y.V., Sukarieh, R., M'Boutchou, M.N. & Sonenberg, N. Mammalian poly(A)-binding protein is a eukaryotic translation initiation factor, which acts via multiple mechanisms. *Genes Dev* **19**, 104-113 (2005).
13. Merrick, W.C. Overview: mechanism of translation initiation in eukaryotes. *Enzyme* **44**, 7-16 (1990).

14. Marintchev, A., Kolupaeva, V.G., Pestova, T.V. & Wagner, G. Mapping the binding interface between human eukaryotic initiation factors 1A and 5B: a new interaction between old partners. *Proc Natl Acad Sci U S A* **100**, 1535-1540 (2003).
15. Dever, T.E. & Green, R. The elongation, termination, and recycling phases of translation in eukaryotes. *Cold Spring Harb Perspect Biol* **4**, a013706 (2012).
16. Glick, B.R., Chladek, S. & Ganoza, M.C. Peptide bond formation stimulated by protein synthesis factor EF-P depends on the aminoacyl moiety of the acceptor. *Eur J Biochem* **97**, 23-28 (1979).
17. Jia, Y., Polunovsky, V., Bitterman, P.B. & Wagner, C.R. Cap-dependent translation initiation factor eIF4E: an emerging anticancer drug target. *Med Res Rev* **32**, 786-814 (2012).
18. Haimov, O., Sinvani, H. & Dikstein, R. Cap-dependent, scanning-free translation initiation mechanisms. *Biochim Biophys Acta* **1849**, 1313-1318 (2015).
19. Thakor, N. & Holcik, M. IRES-mediated translation of cellular messenger RNA operates in eIF2alpha- independent manner during stress. *Nucleic Acids Res* **40**, 541-552 (2012).
20. Martinez-Salas, E., Pineiro, D. & Fernandez, N. Alternative Mechanisms to Initiate Translation in Eukaryotic mRNAs. *Comp Funct Genomics* **2012**, 391546 (2012).
21. Kuyumcu-Martinez, N.M., Van Eden, M.E., Younan, P. & Lloyd, R.E. Cleavage of poly(A)-binding protein by poliovirus 3C protease inhibits host cell translation: a novel mechanism for host translation shutoff. *Mol Cell Biol* **24**, 1779-1790 (2004).
22. Sweeney, T.R., Abaeva, I.S., Pestova, T.V. & Hellen, C.U. The mechanism of translation initiation on Type 1 picornavirus IRESs. *EMBO J* **33**, 76-92 (2014).
23. Komar, A.A. & Hatzoglou, M. Cellular IRES-mediated translation: the war of ITAFs in pathophysiological states. *Cell Cycle* **10**, 229-240 (2011).
24. Marivin, A., Berthelet, J., Plenchette, S. & Dubrez, L. The Inhibitor of Apoptosis (IAPs) in Adaptive Response to Cellular Stress. *Cells* **1**, 711-737 (2012).
25. Sharma, D.K., Bressler, K., Patel, H., Balasingam, N. & Thakor, N. Role of Eukaryotic Initiation Factors during Cellular Stress and Cancer Progression. *J Nucleic Acids* **2016**, 8235121 (2016).
26. Hanson, P.J. *et al.* IRES-Dependent Translational Control during Virus-Induced Endoplasmic Reticulum Stress and Apoptosis. *Front Microbiol* **3**, 92 (2012).



27. Fulda, S., Gorman, A.M., Hori, O. & Samali, A. Cellular stress responses: cell survival and cell death. *Int J Cell Biol* **2010**, 214074 (2010).
28. Holcik, M. & Sonenberg, N. Translational control in stress and apoptosis. *Nat Rev Mol Cell Biol* **6**, 318-327 (2005).
29. Sonenberg, N. & Hinnebusch, A.G. Regulation of translation initiation in eukaryotes: mechanisms and biological targets. *Cell* **136**, 731-745 (2009).
30. Liu, B. & Qian, S.B. Translational reprogramming in cellular stress response. *Wiley Interdiscip Rev RNA* **5**, 301-315 (2014).
31. Richter, J.D. & Sonenberg, N. Regulation of cap-dependent translation by eIF4E inhibitory proteins. *Nature* **433**, 477-480 (2005).
32. Rosettani, P., Knapp, S., Vismara, M.G., Rusconi, L. & Cameron, A.D. Structures of the human eIF4E homologous protein, h4EHP, in its m7GTP-bound and unliganded forms. *J Mol Biol* **368**, 691-705 (2007).
33. Svitkin, Y.V. *et al.* Eukaryotic translation initiation factor 4E availability controls the switch between cap-dependent and internal ribosomal entry site-mediated translation. *Mol Cell Biol* **25**, 10556-10565 (2005).
34. Cho, P.F. *et al.* A new paradigm for translational control: inhibition via 5'-3' mRNA tethering by Bicoid and the eIF4E cognate 4EHP. *Cell* **121**, 411-423 (2005).
35. Bhat, M. *et al.* Targeting the translation machinery in cancer. *Nat Rev Drug Discov* **14**, 261-278 (2015).
36. Jiang, H.Y. & Wek, R.C. Phosphorylation of the alpha-subunit of the eukaryotic initiation factor-2 (eIF2alpha) reduces protein synthesis and enhances apoptosis in response to proteasome inhibition. *J Biol Chem* **280**, 14189-14202 (2005).
37. Sudhakar, A. *et al.* Phosphorylation of serine 51 in initiation factor 2 alpha (eIF2 alpha) promotes complex formation between eIF2 alpha(P) and eIF2B and causes inhibition in the guanine nucleotide exchange activity of eIF2B. *Biochemistry* **39**, 12929-12938 (2000).
38. Pakos-Zebrucka, K. *et al.* The integrated stress response. *EMBO Rep* **17**, 1374-1395 (2016).
39. Harding, H.P. *et al.* An integrated stress response regulates amino acid metabolism and resistance to oxidative stress. *Mol Cell* **11**, 619-633 (2003).
40. Brostrom, C.O., Prostko, C.R., Kaufman, R.J. & Brostrom, M.A. Inhibition of translational initiation by activators of the glucose-regulated stress protein and heat

- shock protein stress response systems. Role of the interferon-inducible double-stranded RNA-activated eukaryotic initiation factor 2alpha kinase. *J Biol Chem* **271**, 24995-25002 (1996).
41. Rzymiski, T. *et al.* Regulation of autophagy by ATF4 in response to severe hypoxia. *Oncogene* **29**, 4424-4435 (2010).
  42. Baird, T.D. & Wek, R.C. Eukaryotic initiation factor 2 phosphorylation and translational control in metabolism. *Adv Nutr* **3**, 307-321 (2012).
  43. Hinnebusch, A.G. Molecular mechanism of scanning and start codon selection in eukaryotes. *Microbiol Mol Biol Rev* **75**, 434-467, first page of table of contents (2011).
  44. Lee, Y.Y., Cevallos, R.C. & Jan, E. An upstream open reading frame regulates translation of GADD34 during cellular stresses that induce eIF2alpha phosphorylation. *J Biol Chem* **284**, 6661-6673 (2009).
  45. Palam, L.R., Baird, T.D. & Wek, R.C. Phosphorylation of eIF2 facilitates ribosomal bypass of an inhibitory upstream ORF to enhance CHOP translation. *J Biol Chem* **286**, 10939-10949 (2011).
  46. Chan, C.P., Kok, K.H., Tang, H.M., Wong, C.M. & Jin, D.Y. Internal ribosome entry site-mediated translational regulation of ATF4 splice variant in mammalian unfolded protein response. *Biochim Biophys Acta* **1833**, 2165-2175 (2013).
  47. Vattem, K.M. & Wek, R.C. Reinitiation involving upstream ORFs regulates ATF4 mRNA translation in mammalian cells. *Proc Natl Acad Sci U S A* **101**, 11269-11274 (2004).
  48. Averous, J. *et al.* Amino acid deprivation regulates the stress-inducible gene p8 via the GCN2/ATF4 pathway. *Biochem Biophys Res Commun* **413**, 24-29 (2011).
  49. Dey, S. *et al.* Both transcriptional regulation and translational control of ATF4 are central to the integrated stress response. *J Biol Chem* **285**, 33165-33174 (2010).
  50. Ryoo, H.D. & Vasudevan, D. Two distinct nodes of translational inhibition in the Integrated Stress Response. *BMB Rep* **50**, 539-545 (2017).
  51. Riley, A., Jordan, L.E. & Holcik, M. Distinct 5' UTRs regulate XIAP expression under normal growth conditions and during cellular stress. *Nucleic Acids Res* **38**, 4665-4674 (2010).
  52. Harding, H.P., Zhang, Y. & Ron, D. Protein translation and folding are coupled by an endoplasmic-reticulum-resident kinase. *Nature* **397**, 271-274 (1999).

53. Garcia, M.A., Meurs, E.F. & Esteban, M. The dsRNA protein kinase PKR: virus and cell control. *Biochimie* **89**, 799-811 (2007).
54. Wek, R.C., Jiang, H.Y. & Anthony, T.G. Coping with stress: eIF2 kinases and translational control. *Biochem Soc Trans* **34**, 7-11 (2006).
55. Donnelly, N., Gorman, A.M., Gupta, S. & Samali, A. The eIF2alpha kinases: their structures and functions. *Cell Mol Life Sci* **70**, 3493-3511 (2013).
56. Clemens, M.J. & Elia, A. The double-stranded RNA-dependent protein kinase PKR: structure and function. *J Interferon Cytokine Res* **17**, 503-524 (1997).
57. Zhang, F. *et al.* Binding of double-stranded RNA to protein kinase PKR is required for dimerization and promotes critical autophosphorylation events in the activation loop. *J Biol Chem* **276**, 24946-24958 (2001).
58. Balachandran, S. *et al.* Essential role for the dsRNA-dependent protein kinase PKR in innate immunity to viral infection. *Immunity* **13**, 129-141 (2000).
59. Lee, S.B. & Esteban, M. The interferon-induced double-stranded RNA-activated human p68 protein kinase inhibits the replication of vaccinia virus. *Virology* **193**, 1037-1041 (1993).
60. Reineke, L.C. & Lloyd, R.E. The stress granule protein G3BP1 recruits protein kinase R to promote multiple innate immune antiviral responses. *J Virol* **89**, 2575-2589 (2015).
61. Saelens, X., Kalai, M. & Vandenabeele, P. Translation inhibition in apoptosis: caspase-dependent PKR activation and eIF2-alpha phosphorylation. *J Biol Chem* **276**, 41620-41628 (2001).
62. Castilho, B.A. *et al.* Keeping the eIF2 alpha kinase Gcn2 in check. *Biochim Biophys Acta* **1843**, 1948-1968 (2014).
63. Deng, J. *et al.* Activation of GCN2 in UV-irradiated cells inhibits translation. *Curr Biol* **12**, 1279-1286 (2002).
64. Korennykh, A. & Walter, P. Structural basis of the unfolded protein response. *Annu Rev Cell Dev Biol* **28**, 251-277 (2012).
65. Wang, M. & Kaufman, R.J. Protein misfolding in the endoplasmic reticulum as a conduit to human disease. *Nature* **529**, 326-335 (2016).
66. Han, A.P. *et al.* Heme-regulated eIF2alpha kinase (HRI) is required for translational regulation and survival of erythroid precursors in iron deficiency. *EMBO J* **20**, 6909-6918 (2001).

67. Lu, L., Han, A.P. & Chen, J.J. Translation initiation control by heme-regulated eukaryotic initiation factor 2alpha kinase in erythroid cells under cytoplasmic stresses. *Mol Cell Biol* **21**, 7971-7980 (2001).
68. Hamanaka, R.B., Bennett, B.S., Cullinan, S.B. & Diehl, J.A. PERK and GCN2 contribute to eIF2alpha phosphorylation and cell cycle arrest after activation of the unfolded protein response pathway. *Mol Biol Cell* **16**, 5493-5501 (2005).
69. Lehman, S.L., Ryeom, S. & Koumenis, C. Signaling through alternative Integrated Stress Response pathways compensates for GCN2 loss in a mouse model of soft tissue sarcoma. *Sci Rep* **5**, 11781 (2015).
70. Novoa, I., Zeng, H., Harding, H.P. & Ron, D. Feedback inhibition of the unfolded protein response by GADD34-mediated dephosphorylation of eIF2alpha. *J Cell Biol* **153**, 1011-1022 (2001).
71. Marciniak, S.J. *et al.* CHOP induces death by promoting protein synthesis and oxidation in the stressed endoplasmic reticulum. *Genes Dev* **18**, 3066-3077 (2004).
72. Ohoka, N., Yoshii, S., Hattori, T., Onozaki, K. & Hayashi, H. TRB3, a novel ER stress-inducible gene, is induced via ATF4-CHOP pathway and is involved in cell death. *EMBO J* **24**, 1243-1255 (2005).
73. Wang, Q. *et al.* ERAD inhibitors integrate ER stress with an epigenetic mechanism to activate BH3-only protein NOXA in cancer cells. *Proc Natl Acad Sci U S A* **106**, 2200-2205 (2009).
74. B'Chir, W. *et al.* The eIF2alpha/ATF4 pathway is essential for stress-induced autophagy gene expression. *Nucleic Acids Res* **41**, 7683-7699 (2013).
75. Galehdar, Z. *et al.* Neuronal apoptosis induced by endoplasmic reticulum stress is regulated by ATF4-CHOP-mediated induction of the Bcl-2 homology 3-only member PUMA. *J Neurosci* **30**, 16938-16948 (2010).
76. Zou, W., Yue, P., Khuri, F.R. & Sun, S.Y. Coupling of endoplasmic reticulum stress to CDDO-Me-induced up-regulation of death receptor 5 via a CHOP-dependent mechanism involving JNK activation. *Cancer Res* **68**, 7484-7492 (2008).
77. Armstrong, J.L., Flockhart, R., Veal, G.J., Lovat, P.E. & Redfern, C.P. Regulation of endoplasmic reticulum stress-induced cell death by ATF4 in neuroectodermal tumor cells. *J Biol Chem* **285**, 6091-6100 (2010).
78. Hiramatsu, N. *et al.* Translational and posttranslational regulation of XIAP by eIF2alpha and ATF4 promotes ER stress-induced cell death during the unfolded protein response. *Mol Biol Cell* **25**, 1411-1420 (2014).

79. Boyce, M. *et al.* A selective inhibitor of eIF2 $\alpha$  dephosphorylation protects cells from ER stress. *Science* **307**, 935-939 (2005).
80. Jousse, C. *et al.* Inhibition of a constitutive translation initiation factor 2 $\alpha$  phosphatase, CReP, promotes survival of stressed cells. *J Cell Biol* **163**, 767-775 (2003).
81. Kojima, E. *et al.* The function of GADD34 is a recovery from a shutoff of protein synthesis induced by ER stress: elucidation by GADD34-deficient mice. *FASEB J* **17**, 1573-1575 (2003).
82. Novoa, I. *et al.* Stress-induced gene expression requires programmed recovery from translational repression. *EMBO J* **22**, 1180-1187 (2003).
83. Shi, W. *et al.* GADD34-PP1c recruited by Smad7 dephosphorylates TGF $\beta$  type I receptor. *J Cell Biol* **164**, 291-300 (2004).
84. Farook, J.M. *et al.* GADD34 induces cell death through inactivation of Akt following traumatic brain injury. *Cell Death Dis* **4**, e754 (2013).
85. Hamanaka, R.B., Bobrovnikova-Marjon, E., Ji, X., Liebhaber, S.A. & Diehl, J.A. PERK-dependent regulation of IAP translation during ER stress. *Oncogene* **28**, 910-920 (2009).
86. Bobrovnikova-Marjon, E. *et al.* PERK promotes cancer cell proliferation and tumor growth by limiting oxidative DNA damage. *Oncogene* **29**, 3881-3895 (2010).
87. Yuan, J. & Kroemer, G. Alternative cell death mechanisms in development and beyond. *Genes Dev* **24**, 2592-2602 (2010).
88. Gavrilescu, L.C. & Denkers, E.Y. Apoptosis and the balance of homeostatic and pathologic responses to protozoan infection. *Infect Immun* **71**, 6109-6115 (2003).
89. Roos, W.P. & Kaina, B. DNA damage-induced cell death by apoptosis. *Trends Mol Med* **12**, 440-450 (2006).
90. Alnemri, E.S. *et al.* Human ICE/CED-3 protease nomenclature. *Cell* **87**, 171 (1996).
91. Shi, Y. Caspase activation, inhibition, and reactivation: a mechanistic view. *Protein Sci* **13**, 1979-1987 (2004).
92. Li, J. & Yuan, J. Caspases in apoptosis and beyond. *Oncogene* **27**, 6194-6206 (2008).
93. Elmore, S. Apoptosis: a review of programmed cell death. *Toxicol Pathol* **35**, 495-516 (2007).

94. Gulbins, E., Dreschers, S. & Bock, J. Role of mitochondria in apoptosis. *Exp Physiol* **88**, 85-90 (2003).
95. Riedl, S.J. & Salvesen, G.S. The apoptosome: signalling platform of cell death. *Nat Rev Mol Cell Biol* **8**, 405-413 (2007).
96. Hoetelmans, R. *et al.* Bcl-2 and Bax proteins are present in interphase nuclei of mammalian cells. *Cell Death Differ* **7**, 384-392 (2000).
97. Martinou, J.C. & Youle, R.J. Mitochondria in apoptosis: Bcl-2 family members and mitochondrial dynamics. *Dev Cell* **21**, 92-101 (2011).
98. Srinivasula, S.M. *et al.* Molecular determinants of the caspase-promoting activity of Smac/DIABLO and its role in the death receptor pathway. *J Biol Chem* **275**, 36152-36157 (2000).
99. Lauber, K. *et al.* The adapter protein apoptotic protease-activating factor-1 (Apaf-1) is proteolytically processed during apoptosis. *J Biol Chem* **276**, 29772-29781 (2001).
100. Parrish, A.B., Freel, C.D. & Kornbluth, S. Cellular mechanisms controlling caspase activation and function. *Cold Spring Harb Perspect Biol* **5** (2013).
101. Susin, S.A. *et al.* Molecular characterization of mitochondrial apoptosis-inducing factor. *Nature* **397**, 441-446 (1999).
102. Li, L.Y., Luo, X. & Wang, X. Endonuclease G is an apoptotic DNase when released from mitochondria. *Nature* **412**, 95-99 (2001).
103. Guicciardi, M.E. & Gores, G.J. Life and death by death receptors. *FASEB J* **23**, 1625-1637 (2009).
104. Ozoren, N. & El-Deiry, W.S. Cell surface Death Receptor signaling in normal and cancer cells. *Semin Cancer Biol* **13**, 135-147 (2003).
105. Kantari, C. & Walczak, H. Caspase-8 and bid: caught in the act between death receptors and mitochondria. *Biochim Biophys Acta* **1813**, 558-563 (2011).
106. Wang, S. & El-Deiry, W.S. TRAIL and apoptosis induction by TNF-family death receptors. *Oncogene* **22**, 8628-8633 (2003).
107. Jin, Z. & El-Deiry, W.S. Distinct signaling pathways in TRAIL- versus tumor necrosis factor-induced apoptosis. *Mol Cell Biol* **26**, 8136-8148 (2006).
108. Berthelet, J. & Dubrez, L. Regulation of Apoptosis by Inhibitors of Apoptosis (IAPs). *Cells* **2**, 163-187 (2013).

109. Clem, R.J. & Miller, L.K. Control of programmed cell death by the baculovirus genes p35 and iap. *Mol Cell Biol* **14**, 5212-5222 (1994).
110. Riedl, S.J. & Shi, Y. Molecular mechanisms of caspase regulation during apoptosis. *Nat Rev Mol Cell Biol* **5**, 897-907 (2004).
111. Hay, B.A. Understanding IAP function and regulation: a view from Drosophila. *Cell Death Differ* **7**, 1045-1056 (2000).
112. Hunter, A.M., LaCasse, E.C. & Korneluk, R.G. The inhibitors of apoptosis (IAPs) as cancer targets. *Apoptosis* **12**, 1543-1568 (2007).
113. Altieri, D.C. Survivin and IAP proteins in cell-death mechanisms. *Biochem J* **430**, 199-205 (2010).
114. Silke, J. *et al.* Determination of cell survival by RING-mediated regulation of inhibitor of apoptosis (IAP) protein abundance. *Proc Natl Acad Sci U S A* **102**, 16182-16187 (2005).
115. Scott, F.L. *et al.* XIAP inhibits caspase-3 and -7 using two binding sites: evolutionarily conserved mechanism of IAPs. *EMBO J* **24**, 645-655 (2005).
116. Takahashi, R. *et al.* A single BIR domain of XIAP sufficient for inhibiting caspases. *J Biol Chem* **273**, 7787-7790 (1998).
117. Samuel, T. *et al.* Distinct BIR domains of cIAP1 mediate binding to and ubiquitination of tumor necrosis factor receptor-associated factor 2 and second mitochondrial activator of caspases. *J Biol Chem* **281**, 1080-1090 (2006).
118. Creagh, E.M., Murphy, B.M., Duriez, P.J., Duckett, C.S. & Martin, S.J. Smac/Diablo antagonizes ubiquitin ligase activity of inhibitor of apoptosis proteins. *J Biol Chem* **279**, 26906-26914 (2004).
119. Kasof, G.M. & Gomes, B.C. Livin, a novel inhibitor of apoptosis protein family member. *J Biol Chem* **276**, 3238-3246 (2001).
120. Akl, H. *et al.* A dual role for the anti-apoptotic Bcl-2 protein in cancer: mitochondria versus endoplasmic reticulum. *Biochim Biophys Acta* **1843**, 2240-2252 (2014).
121. Westphal, D., Dewson, G., Czabotar, P.E. & Kluck, R.M. Molecular biology of Bax and Bak activation and action. *Biochim Biophys Acta* **1813**, 521-531 (2011).
122. Safa, A.R. c-FLIP, a master anti-apoptotic regulator. *Exp Oncol* **34**, 176-184 (2012).
123. Micheau, O., Lens, S., Gaide, O., Alevizopoulos, K. & Tschopp, J. NF-kappaB signals induce the expression of c-FLIP. *Mol Cell Biol* **21**, 5299-5305 (2001).

124. Wong, R.S. Apoptosis in cancer: from pathogenesis to treatment. *J Exp Clin Cancer Res* **30**, 87 (2011).
125. Ruggero, D. Translational control in cancer etiology. *Cold Spring Harb Perspect Biol* **5** (2013).
126. Gray, N.K. & Wickens, M. Control of translation initiation in animals. *Annu Rev Cell Dev Biol* **14**, 399-458 (1998).
127. Nupponen, N.N. *et al.* Amplification and overexpression of p40 subunit of eukaryotic translation initiation factor 3 in breast and prostate cancer. *Am J Pathol* **154**, 1777-1783 (1999).
128. Doldan, A. *et al.* Loss of the eukaryotic initiation factor 3f in pancreatic cancer. *Mol Carcinog* **47**, 235-244 (2008).
129. Sorrells, D.L. *et al.* Detection of eIF4E gene amplification in breast cancer by competitive PCR. *Ann Surg Oncol* **5**, 232-237 (1998).
130. Bauer, C. *et al.* Translation initiation factor eIF-4G is immunogenic, overexpressed, and amplified in patients with squamous cell lung carcinoma. *Cancer* **92**, 822-829 (2001).
131. Rhoads, R.E. miRNA regulation of the translational machinery. Preface. *Prog Mol Subcell Biol* **50**, v-vi (2010).
132. Dmitriev, S.E. *et al.* GTP-independent tRNA delivery to the ribosomal P-site by a novel eukaryotic translation factor. *J Biol Chem* **285**, 26779-26787 (2010).
133. Leipe, D.D., Wolf, Y.I., Koonin, E.V. & Aravind, L. Classification and evolution of P-loop GTPases and related ATPases. *J Mol Biol* **317**, 41-72 (2002).
134. Koller-Eichhorn, R. *et al.* Human OLA1 defines an ATPase subfamily in the Obg family of GTP-binding proteins. *J Biol Chem* **282**, 19928-19937 (2007).
135. Zhang, J., Rubio, V., Lieberman, M.W. & Shi, Z.Z. OLA1, an Obg-like ATPase, suppresses antioxidant response via nontranscriptional mechanisms. *Proc Natl Acad Sci U S A* **106**, 15356-15361 (2009).
136. Chen, H. *et al.* OLA1 regulates protein synthesis and integrated stress response by inhibiting eIF2 ternary complex formation. *Sci Rep* **5**, 13241 (2015).
137. Mao, R.F. *et al.* OLA1 protects cells in heat shock by stabilizing HSP70. *Cell Death Dis* **4**, e491 (2013).



138. Takahashi, M. *et al.* OLA1 gene sequencing in patients with BRCA1/2 mutation-negative suspected hereditary breast and ovarian cancer. *Breast Cancer* **24**, 336-340 (2017).
139. Matsuzawa, A. *et al.* The BRCA1/BARD1-interacting protein OLA1 functions in centrosome regulation. *Mol Cell* **53**, 101-114 (2014).
140. Sun, H. *et al.* DOC45, a novel DNA damage-regulated nucleocytoplasmic ATPase that is overexpressed in multiple human malignancies. *Mol Cancer Res* **8**, 57-66 (2010).
141. Park, M.S. & Koff, A. Overview of the cell cycle. *Curr Protoc Cell Biol* **Chapter 8**, Unit 8 1 (2001).
142. Barnum, K.J. & O'Connell, M.J. Cell cycle regulation by checkpoints. *Methods Mol Biol* **1170**, 29-40 (2014).
143. Ding, Z. *et al.* OLA1, a Translational Regulator of p21, Maintains Optimal Cell Proliferation Necessary for Developmental Progression. *Mol Cell Biol* **36**, 2568-2582 (2016).
144. Noh, H.J. *et al.* CHOP down-regulates cFLIP(L) expression by promoting ubiquitin/proteasome-mediated cFLIP(L) degradation. *J Cell Biochem* **113**, 3692-3700 (2012).
145. Qi, Y. & Xia, P. Cellular inhibitor of apoptosis protein-1 (cIAP1) plays a critical role in beta-cell survival under endoplasmic reticulum stress: promoting ubiquitination and degradation of C/EBP homologous protein (CHOP). *J Biol Chem* **287**, 32236-32245 (2012).
146. Makki, J. Diversity of Breast Carcinoma: Histological Subtypes and Clinical Relevance. *Clin Med Insights Pathol* **8**, 23-31 (2015).
147. Zhang, J.W., Rubio, V., Zheng, S. & Shi, Z.Z. Knockdown of OLA1, a regulator of oxidative stress response, inhibits motility and invasion of breast cancer cells. *J Zhejiang Univ Sci B* **10**, 796-804 (2009).
148. Ruiz Esparza-Garrido, R. *et al.* Breast cancer cell line MDA-MB-231 miRNA profile expression after BIK interference: BIK involvement in autophagy. *Tumour Biol* **37**, 6749-6759 (2016).
149. Holliday, D.L. & Speirs, V. Choosing the right cell line for breast cancer research. *Breast Cancer Res* **13**, 215 (2011).
150. Chiba, N. [BRCA1-interacting protein OLA1 functions in the maintenance of genome integrity by centrosome regulation]. *Seikagaku* **87**, 741-743 (2015).

151. Graber, T.E. & Holcik, M. Distinct roles for the cellular inhibitors of apoptosis proteins 1 and 2. *Cell Death Dis* **2**, e135 (2011).
152. Safa, A.R. Roles of c-FLIP in Apoptosis, Necroptosis, and Autophagy. *J Carcinog Mutagen Suppl* **6** (2013).
153. Gaudette, B.T., Iwakoshi, N.N. & Boise, L.H. Bcl-xL protein protects from C/EBP homologous protein (CHOP)-dependent apoptosis during plasma cell differentiation. *J Biol Chem* **289**, 23629-23640 (2014).
154. Yang, F., Teves, S.S., Kemp, C.J. & Henikoff, S. Doxorubicin, DNA torsion, and chromatin dynamics. *Biochim Biophys Acta* **1845**, 84-89 (2014).
155. Srivastava, R.K. TRAIL/Apo-2L: mechanisms and clinical applications in cancer. *Neoplasia* **3**, 535-546 (2001).
156. Herceg, Z. & Wang, Z.Q. Functions of poly(ADP-ribose) polymerase (PARP) in DNA repair, genomic integrity and cell death. *Mutat Res* **477**, 97-110 (2001).
157. Anania, V.G. *et al.* Uncovering a Dual Regulatory Role for Caspases During Endoplasmic Reticulum Stress-induced Cell Death. *Mol Cell Proteomics* **15**, 2293-2307 (2016).
158. McIlwain, D.R., Berger, T. & Mak, T.W. Caspase functions in cell death and disease. *Cold Spring Harb Perspect Biol* **7** (2015).
159. Portt, L., Norman, G., Clapp, C., Greenwood, M. & Greenwood, M.T. Anti-apoptosis and cell survival: a review. *Biochim Biophys Acta* **1813**, 238-259 (2011).
160. Zaremba, T., Thomas, H., Cole, M., Plummer, E.R. & Curtin, N.J. Doxorubicin-induced suppression of poly(ADP-ribose) polymerase-1 (PARP-1) activity and expression and its implication for PARP inhibitors in clinical trials. *Cancer Chemother Pharmacol* **66**, 807-812 (2010).
161. Riccardi, C. & Nicoletti, I. Analysis of apoptosis by propidium iodide staining and flow cytometry. *Nat Protoc* **1**, 1458-1461 (2006).
162. Kikkawa, Y. *et al.* Down-regulation of cell adhesion via rho-associated protein kinase (ROCK) pathway promotes tumor cell migration on laminin-511. *Exp Cell Res* **344**, 76-85 (2016).
163. Lu, P.D., Harding, H.P. & Ron, D. Translation reinitiation at alternative open reading frames regulates gene expression in an integrated stress response. *J Cell Biol* **167**, 27-33 (2004).

164. Teske, B.F. *et al.* CHOP induces activating transcription factor 5 (ATF5) to trigger apoptosis in response to perturbations in protein homeostasis. *Mol Biol Cell* **24**, 2477-2490 (2013).
165. Hetz, C. The unfolded protein response: controlling cell fate decisions under ER stress and beyond. *Nat Rev Mol Cell Biol* **13**, 89-102 (2012).
166. Rodriguez, D., Rojas-Rivera, D. & Hetz, C. Integrating stress signals at the endoplasmic reticulum: The BCL-2 protein family rheostat. *Biochim Biophys Acta* **1813**, 564-574 (2011).
167. Yamaguchi, H. & Wang, H.G. CHOP is involved in endoplasmic reticulum stress-induced apoptosis by enhancing DR5 expression in human carcinoma cells. *J Biol Chem* **279**, 45495-45502 (2004).
168. Rerole, A.L., Jego, G. & Garrido, C. Hsp70: anti-apoptotic and tumorigenic protein. *Methods Mol Biol* **787**, 205-230 (2011).
169. Mahoney, D.J. *et al.* Both cIAP1 and cIAP2 regulate TNFalpha-mediated NF-kappaB activation. *Proc Natl Acad Sci U S A* **105**, 11778-11783 (2008).
170. Taylor, S.C., Berkelman, T., Yadav, G. & Hammond, M. A defined methodology for reliable quantification of Western blot data. *Mol Biotechnol* **55**, 217-226 (2013).
171. Suzuki-Karasaki, Y. *et al.* Distinct effects of TRAIL on the mitochondrial network in human cancer cells and normal cells: role of plasma membrane depolarization. *Oncotarget* **6**, 21572-21588 (2015).
172. Callis, J. The ubiquitination machinery of the ubiquitin system. *Arabidopsis Book* **12**, e0174 (2014).
173. Sambrook, J. & Russell, D.W. Detection of Protein-Protein Interactions Using the GST Fusion Protein Pulldown Technique. *CSH Protoc* **2006** (2006).
174. Regan, J.N. *et al.* Osteolytic Breast Cancer Causes Skeletal Muscle Weakness in an Immunocompetent Syngeneic Mouse Model. *Front Endocrinol (Lausanne)* **8**, 358 (2017).